Geochemical characterisation of sediment, shale and crude oil from the Indian part of southern Bengal Basin for reconstruction of depositional environment

Supervisor

Dr. Supriyo Kumar Das

Synopsis of Thesis

By

Pravat Kumar Behera

Senior Research Fellow

Department of Geology

Presidency University

Reg. No.: R-19RS215110199

Geochemical characterisation of sediment, shale and crude oil from the Indian part of southern Bengal Basin for reconstruction of depositional environment

Introduction

The Bengal Basin, a complex foreland basin (Mukherjee et al., 2009), is situated at the conjunction of the Indian craton to the west, the Himalayan belt and Shilong massif to the north and the Indo-Burman ranges to the east (Uddin and Lundberg, 1998). Tectonically, the basin is divided into two broad parts by the Eocene Hinge zone (a deep seismic hinge zone): a Stable shelf (Indian platform) to the northwest and west, and the deeper part of the basin (Bengal foredeep) in the south and east (Sengupta, 1966; Uddin and Lundberg, 1998). The basin shows noticeable variability in Neogene sediment thickness, indicating a complicated tectonic and depositional history (Hossain et al., 2019). Sedimentation in the basin started in the late Eocene (Uddin and Lundberg, 1998; Najman et al., 2008). A major phase of clastic sedimentation from the northeast, beginning in the early Miocene, led to the formation of the major Mio-Pliocene delta complex (Uddin, 1990). The Miocene-Pliocene-Pleistocene depositional environments are dominated by brackish-estuarine-deltaic conditions and marginal marine conditions inferred from a micropaleontological study in the Jessore depression and Surma Basin in Bangladesh (Banerji, 1984). The Ganges and Brahmaputra rivers transport the clastic sediments from the Himalayas and deposit them in the Ganges-Brahmaputra deltaic system (Hossain et al., 2009). Stratigraphy, sedimentation and tectonic history of the basin have been studied in detail in the northeastern part, revealing that Miocene sedimentation has changed from flysch to molasse (Alam, 1989; Johnson and Alam, 1991). Also, a tide-dominated shallow marine sedimentation during the Miocene in the southeastern Bengal Basin has been postulated (Alam, 1995). Hossain et al. (2009) have inferred anoxic to sub-oxic depositional conditions of the Miocene-Pleistocene sediments with decreasing terrestrial higher plant organic matter (OM) input in the Sylhet Basin (a sub-basin of the Bengal Basin in Bangladesh) using elemental carbon (C), nitrogen (N), sulfur (S), Rock-Eval pyrolysis and gas chromatography-mass spectroscopy (GC-MS). The thick (±22 km) sedimentary succession of the early Cretaceous to Holocene led to significant attention to hydrocarbon exploration in the Bengal Basin (Curray, 1991; Curray and Munasinghe, 1991). Hydrocarbon exploration has been extensively carried out by the Bangladesh Oil, Gas and Mineral Corporation (BOGMC, 1997) in the last few decades, and an economic quantity of natural gas has been reported in the Bangladesh section

of the Bengal Basin (Bengal Foredeep), where terrestrial OM at an early maturation stage is considered as the source of the gas (Imam and Hussain, 2002; Islam, 2009). The Indian section of the Bengal Basin is also considered as geologically prospective for hydrocarbon generation, and over 50 wells have been drilled during the last three decades under the Indo-Stanvac Petroleum Project and by the Oil and Natural Gas Corporation (ONGC) Limited (Banerji et al., 1990). Most gas indications in the drilled wells under the Indo-Stanvac Petroleum Project have been associated with Miocene sediments (Ramaswamy, 1962). The ONGC has reported natural gas from several deeper (> 2000 m) wells in West Bengal (Directorate General of Hydrocarbons, 2019) although, unlike Bangladesh, published reports on the paleodepositional conditions and source and maturity of sedimentary OM in the Indian section of the Bengal Basin are rare (e.g., Babu, 1976; Roybarman, 1984; Bastia, 2006).

The objectives of the present study were 1) to evaluate the sources and depositional environment of the OM in the deep Bengal Basin shales and crude oil by studying the stable isotopes of organic carbon ($\delta^{13}C$), nitrogen ($\delta^{15}N$), sulphur ($\delta^{34}S$) and hydrogen ($\delta^{2}H$), elemental C and N, *n*-alkanes, isoprenoid alkane and polycyclic aromatic hydrocarbon (PAH) distribution, and kerogen maturity. 2) to understand the biogenic methane production in the deeper Bengal Basin sediments. 3) to study the $\delta^{13}C$, C and N characteristics of present-day delta and Pliestocene Lower Bengal Fan sediments for a better understanding of past processes.

The Bengal Basin

The Bengal Basin (Fig. 1) is one of the world's largest fluvial-deltaic basins (~200,000 km^2; Alam et al., 2003). The peripheral foreland basin is situated at the confluence of the Brahmaputra and Ganga rivers. The Bengal Fan, Earth's largest deep-sea fan complex (Rea, 1992), is further developed into the Bay of Bengal (Morgan and McIntire, 1959; Babu, 1976; Allison, 1998). The basin lies in the Himalayan foreland at the junction of the Burmese, Eurasian and Indian plates (Mukherjee et al., 2009). Drilling in the Bengal Basin has revealed sedimentary sequences ranging in age from Middle-Upper Cretaceous to recent (Basu, 1962; DGH). Sengupta (1966) summarises that the depositional environment of the Bengal Basin has changed sharply to a foredeep from a stable shelf condition. Eocene hinge zone separates the two depositional environments (Mukherjee et al., 2009). Gondwana basement underlies the Bengal Basin sediments, and the thickness of the sediments varies between the foredeep (> 16

km) and stable shelf (8 km). The basin was formed during the late Jurassic period and major tectonic movements, such as the Dauki fault and Naga thrust occurred during the Late

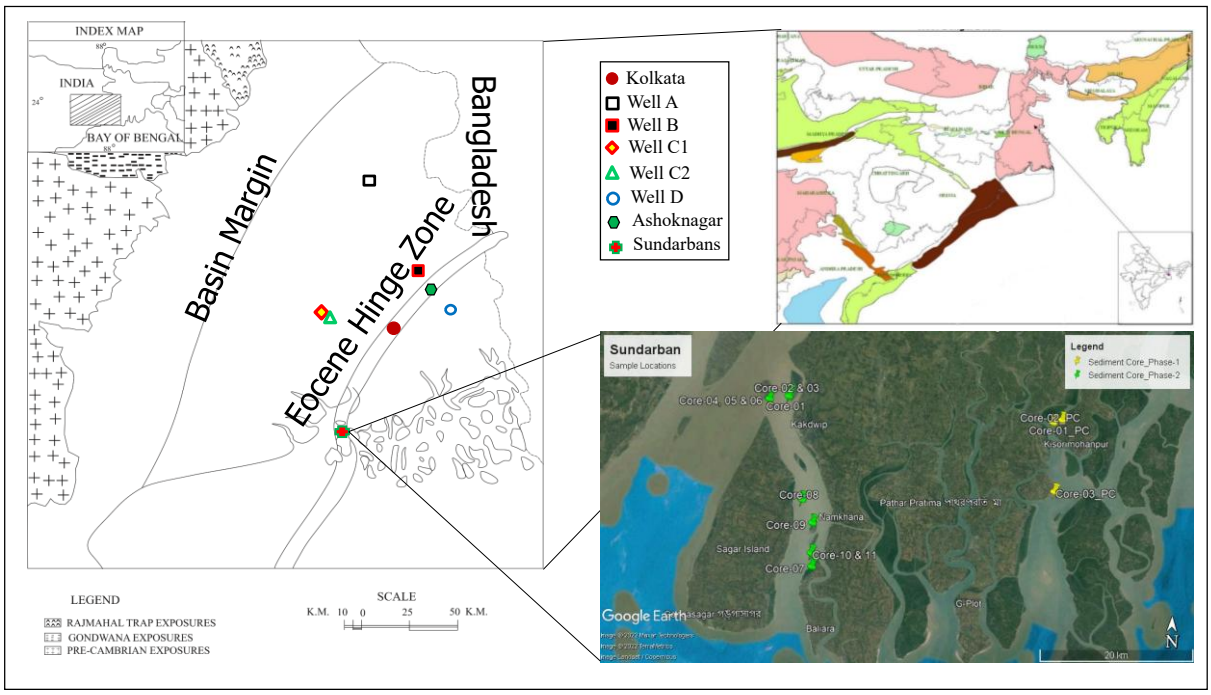

Fig. 1. Location of sampling sites.

Cretaceous, Eocene and Miocene, with the regression of the sea during the late Miocene and early Pliocene (Sengupta, 1966). The Pleistocene and Pliocene sequences in the Bengal Basin primarily belong to the Ranaghat Formation and mostly contain claystone, siltstone and pebbly sandstone, whereas the Miocene Debagram and the Pandua Formations are characterised by claystone, siltstone, sandstone and shale (Banerji, 1984; Alam et al., 2003). The Ranaghat Formation is characteristic of marginal marine with occasional inter-deltaic settings, while the Debagram Formation exhibits a mixed estuarine to marginal deltaic facies character (Banerji, 1984). On the contrary, the presence of planktonic and benthic foraminifera in the Pandua Formation indicates a short span of marine transgression during the Miocene (Banerji, 1984).

Sample and Methods

The Keshava Deva Malaviya Institute of Petroleum and Exploration (KDMIPE) and ONGC provided 93 cutting shale samples from 5 wells (Fig. 1). The MBA Basin of ONGC in Kolkata provided the Ashokanagr crude oil. Recent delta sediments were collected from Sundarbans (Fig. 1; Table 2), West Bengal. Lower Bengal Fan sediments from holes U1451, U1449 and

U1452 collected during the International Ocean Discovery Programme (IODP) Expedition 354 were issued to Dr SK Das.

Rock-Eval pyrolysis

The cutting shale samples' free hydrocarbons (S_1) and thermogenic hydrocarbons (S_2) were measured using a Rock-Eval 6 pyrolyser, Turbo version (Vinci Technologies) at the National Geophysical Research Institute (NGRI) in Hyderabad. The TOC, Tmax (the temperature at which the maximum S_2 was liberated) and the amount of CO_2 produced (S_3) during kerogen pyrolysis in the absence of O_2 were also measured. Oxygen index (OI) and Hydrogen index (HI) were estimated following methods described by Lafargue et al. (1998) and Behar et al. (2001).

FT-IR Spectroscopy

The asphaltene was separated from the Ashoknagar crude oil following the standard protocol IP-143 (Asemani and Rabbani, 2016). MID Infrared (MID-IR) ranging from 4000 cm^{-1} to 400 cm^{-1} spectrums were recorded in transmittance and absorbance mode using a Thermo Scientific NICOLET iS50 FT-IR ATR spectroscopy, with a resolution of 4 cm^{-1}.

NMR spectroscopy

The ^{13}C and ^{1}H of crude oil and asphaltene were measured using an NMR (400 MHZ, Model: Bruker Avance 400) spectrometer. Both samples diluted with $CDCl_3$ and TMS were used as internal spikes.

Stable isotopes ($\delta^{13}C$, $\delta^{15}N$, $\delta^{2}H$ and $\delta^{34}S$) analysis

The TOC, total N (TN) of cutting shale and sediment samples and total sulfur (TS) and total C (TC) content of the whole crude oil were measured using an elemental analyser (EA). An EA, coupled with Europa Scientific 20-20 isotope ratio mass spectrometer (IRMS), was used to analyse the $\delta^{13}C$, $\delta^{2}H$ and $\delta^{34}S$ of whole crude oil and $\delta^{13}C$ of saturate and aromatic fractions and $\delta^{13}C$ and $\delta^{15}N$ of cutting shale and sediment samples. The $\delta^{13}C$ values of the Hole U1452C

sediments are obtained from an article by Weber et al. (2018). The results of the $\delta^{13}C$, $\delta^{15}N$, $\delta^{2}H$ and $\delta^{34}S$ analyses were calculated using the following formula:

$$\delta\ (‰) = [(R_{sample}/R_{standard}) - 1] \times 1000$$

Lipid Biomarkers

Total lipid extracted by using a mixture (3:1, v/v) of dichloromethane and methanol from the homogenised sediments by ultra-sonication (Wu et al., 2014). Aliphatic hydrocarbon fraction was extracted using silica gel column chromatography (Zhang et al., 2004). The aliphatic and aromatic compounds were fractionated from the crude oil by following the protocol described by (Kumar et al., 2021). The *n*-alkanes in shale and sediments were analysed using an Agilent Gas Chromatography-Mass spectrometry (GC-MS) equipped with a HP-ULTRA 2 fused silica capillary column. The GC temperature was programmed from 50 °C-120 °C at 30 °C /min and from 120 °C-310 °C at 6 °C /min, followed by an isothermal period of 25 min. The aliphatic fraction of crude oil and sediment samples was analysed using a Thermo Scientific GC-MS equipped with a DB-5 silica capillary column. The initial oven temperature was programmed at 40 °C with a hold of 5 min. Subsequently, the temperature was increased to 310 °C at 4 °C/min and maintained at 5.5 min. The transfer line temperature was set at 250 °C.

Environmental DNA extraction and analysis

Environmental DNA in four sediment samples (4138-4141 m, 4659-4662 m, 4923-4926 m and 4998-5001 m) of Well D were extracted using the standard protocol as described by Tringe and Rubin (2005) and Liles et al. (2009). The purity and concentration of the DNA were examined using 1% agarose gel horizontal electrophoresis, and the DNA was quantified using a Qubit® dsDNA HS Assay Kit. Samples with TOC content > 1% only had sufficient DNA for downstream molecular analysis. The partial *mcrA* gene and *aprA* fragments were amplified in extracted DNA samples using the McrA and AprA primers (Luton et al., 2002; Meyer and Kuever, 2007). Clone library preparation, sequencing and phylogenetic analysis of generated sequences were performed following methods described by Huber et al. (2004); Rice et al. (2000) and Madeira et al. (2019) and described in details by Behera et al. (2022).

Results

Rock-Eval pyrolysis

The results of the rock-eval pyrolysis is shown in Table 1 below.

Table 1. Rock-Eval pyrolysis data of ONGC shale samples.

Sample ID	S1	S2	S3	Tmax	HI	OI
Well A	0.01-0.11	0.08-0.47	0.48-1.21	311-432	33-141	173-469
Well B	0.01-8.03	0.02-2.01	0.29-1.42	299-609	9-169	88-406
Well C1	0.01-7.32	0.06-1.80	0.34-1.88	298-436	29-140	139-723
Well C1	0.05-14.78	0.09-3.07	0.20-1.65	294-430	69-162	73-348
Well D	0.10-7.88	0.13-2.04	0.39-1.87	296-425	89-176	85-355

Elemental and stable isotope ratio

The elemental and stable isotope ratio of cutting shale samples, crude oil, delta and Bengal Fan sediments are shown in the Table 2.

Table 2. Elemental and isotope ratio of shale, sediment and crude oil samples.

Sample ID	N (%)	TOC (%)	C/N	$\delta^{13}C$	$\delta^{15}N$	$\delta^{34}S$	$\delta^{2}H$
Well A	0.04-0.07	0.22-0.89	4.22-17.31	-25.65 to -23.75	3.02 to 4.43	-	-
Well B	0.02-0.06	0.12-1.22	5.54-24.51	-26.76 to -25.18	3.55 to 4.65	-	-
Well C1	0.02-0.06	0.11-1.44	4.42-31.59	-26.44 to -21.72	3.29 to 4.39	-	-
Well C2	0.02-0.06	0.12-2.29	4.88-41.24	-26.54 to -25.68	3.47 to 3.99	-	-
Well D	0.03-0.06	0.16-1.51	5.39-34.00	-27.01 to -25.99	3.47 to 4.53	-	-
U1449	0.02-0.12	0.20-0.83	5.34-11.49	-22.24 to -18.08	0.02 to 0.12	-	-
U1451	0.04-0.25	0.25-2.26	1.62-28.36	-28.35 to -18.74	-13.7 to 6.9	-	-
U1452	0.03-0.24	0.06-2.16	0.28-15.61	-26.04 to -17.59	4.08 to 10.2	-	-
Nerar Char	0.06-0.19	0.26-0.73	3.41-13.23	-25.00 to -23.25	-	-	-
Baikanthpur Ferry Ghat	0.04-0.07	0.24-0.35	4.48-5.82	-	-	-	-
Burge Island	0.02-0.07	0.43-1.31	6.83-9.96	-	-	-	-
K-Plot	0.03-0.11	0.49-1.12	7.56-23.27	-	-	-	-
Kakrabari Island	0.01-0.10	0.30-2.25	8.20-46.23	-	-	-	-
Whole crude oil	-	67.84	-	-24.77	-	9.00	-107.03
Aliphatic fraction	-	-	-	-24.95	-	-	-
Aromatic fraction	-	-	-	-24.63	-	-	-

FT-IR spectroscopy

The FT-IR spectroscopy data of asphaltene and whole crude oil has been processed in Fityk software to identify different functional groups (Table 3) and measurement of their areas for proxy analysis (Table 4).

Table 3. Functional groups in asphaltene and whole crude oil.

Wavenumbers of the peaks (cm^{-1})	Area under curve (Crude oil)	Area under the curve (Asphaltene)	Type of vibration	Functional group
3140	0.09	0.25	C−H str vib	Aromatic =C-H
2953	1.22	1.45	C−H str vib asym	$-CH_2$
2920	5.43	6.83		
2870	1.03	1.91	C−H str vib sym	$-CH_2$
2850	1.74	2.52		
2730	0.22	0.54	C−O	−CHO, aldehyde
1700		0.30	C=O str vib	ketones
1600	0.08	0.59	C=C str vib	$(ring\ -C\text{-}C-)_{aromatic}$
1460	1.84	1.31	C−H def vib asym	$-CH_3$, $-CH_2$
1380	0.99	1.15	C−H def vib sym	$-CH_3$
1260	0.14	1.43		
1170	0.33	1.65	S=O str vib asym	S=O, sulfoxide
1080	0.14	0.79	S=O str vib sym	S=O, sulfoxide
1030	0.15	0.27		
963	0.12	0.34	C−H def vib	alkenes (C−H)
903	0.03	0.16		
890	0.13	0.21	=C−H def vib	aromatic =C−H
811	0.47	0.08	=C−H def vib	aromatic =C−H
740	0.33	0.47		
721	0.51	0.53	C−H def vib	aliphatic $(CH_2)_n$
701	0.10	0.82		

Asym: asymmetric, sym: symmetric, str: stretching, def: deformation and vib: vibration.

Table 4. Structural parameters calculated from FTIR spectra of asphaltene and crude oil.

Sample Id	A	AL	AR	OX	BS	SS	A_{ali}	SA	AS_1	AS_2	MA	LC_1	LC_2	S_1	S_2
Asphaltene	10.27	0.62	0.11	0.27	0.87	1.31	6.41	0.23	1.11	1.66	1.11	0.04	0.05	0.24	0.09
Crude Oil	6.43	0.81	0.12	0.07	0.54	0.84	5.19	0.23	0.66	1.03	0.66	0.00	0.02	0.20	0.69

The sum of the area $\sum A = (A_{3160}+A_{2962}+A_{2874}+A_{2720}+A_{1600}+A_{1457}+A_{1372}+A_{1160}+A_{1070}+A_{960}+A_{880}+A_{817}+A_{728})$
Aliphatic index (AL) = $(A_{2962}+A_{2874}+A_{1457}+A_{1372}+A_{960}+A_{728})/\sum A$
Aromatic index (AR) = $(A_{3160}+ A_{1600}+ A_{880}+A_{817})/ \sum A$
Oxygen Index (OX) = $(A_{2720+}A_{1700}+ A_{1160}+A_{1070})/ \sum A$
Bending symmetrical index of methyl (BS) = A_{1372}/A_{1457}
Stretching symmetrical index of methylene (SS) = A_{2874}/A_{2962}
The sum of the area ΣA_{ali} represents = = $A_{2962}+A_{2874}+A_{1457}+A_{1372}+A_{960}+A_{728}$
Stretching asymmetrical index of methylene (SA) = $A_{2962}/ \sum A_{ali}$
Alkyl symmetrical index 1 (AS1) = $(A_{2874}+A_{1372})/ (A_{2962}+A_{1457})$
Alkyl symmetrical index 2 (AS2) = A_{2874}/A_{1372}
Methylene asymmetrical index (MA) = A_{2962}/A_{1457}
Long chain index 1 (LC1) = $A_{728}/\Sigma A_{ali}$
Long chain index 2 (LC2) = $A_{960}/\Sigma A_{ali}$
Substitution 1 index (S1) = $A_{880}/ (A_{1600}+A_{880}+A_{817})$
Substitution 2 index (S2) = $A_{817}/ (A_{1600}+A_{880}+A_{817})$

Aliphatic hydrocarbon

Biomarker proxies of cutting shale, sediment and crude oil samples are mentioned in Table 5.

Aromatic Hydrocarbon

Polycyclic aromatic hydrocarbon (PAH) compounds in the crude oil are shown in Table 6. The compounds have been determined based on mass spectra and patterns from the published articles.

Table 5. Biomarker proxies of shale, sediment and crude oil.

Well Name	Sampling interval (m)	CPI-1	CPI-2	TAR	P_{aq}	$1/P_{aq}$	Pr/Ph	Pr/C_{17}	Ph/C_{18}	$(Pr+C_{17})/(Ph+C_{18})$
Well B	1145-1150	1.65	1.08	0.57	0.92	1.09	0.85	3.38	1.89	0.72
	1945-1950	1.10	0.90	0.09	0.95	1.05	0.40	3.27	2.16	0.36
	2540-2545	1.13	0.95	0.15	0.92	1.08	0.81	2.52	1.38	0.66
	3545-3550	1.07	0.81	0.32	0.88	1.14	0.70	2.42	1.45	0.59
Well C-1	2560-2565	1.51	0.99	0.26	0.88	1.14	0.32	0.93	0.82	0.30
Well C-2	1805-1810	1.25	0.92	0.33	0.91	1.10	0.46	1.41	1.64	0.49
	2200-2205	1.03	0.80	0.23	0.91	1.10	0.65	1.67	1.37	0.60
	2700-2705	1.37	0.97	0.27	0.87	1.14	0.58	1.32	0.86	0.47
Well D	3603-3608	1.45	1.07	0.37	0.91	1.10	2.03	2.43	0.73	1.21
	3720-3723	1.46	1.05	0.37	0.90	1.11	2.28	4.19	1.20	1.54
	3801-3804	1.38	0.96	0.37	0.90	1.11	1.70	2.63	1.03	1.19
	3900-3903	1.44	1.03	0.26	0.90	1.11	2.08	1.46	0.55	1.24
	4050-4053	1.50	1.06	0.34	0.91	1.10	1.53	2.19	0.97	1.09
	4138-4141	**1.40**	**1.02**	**0.23**	**0.91**	**1.10**	**1.02**	**0.77**	**0.70**	**0.97**
	4323-4326	1.30	0.91	0.99	0.79	1.27	2.20	4.28	1.15	1.45
	4416-4419	1.44	1.02	0.63	0.83	1.20	2.53	3.05	0.73	1.42
	4500-4503	1.40	1.00	0.61	0.80	1.24	2.32	3.95	0.98	1.44
	4659-4662	**1.42**	**1.03**	**0.96**	**0.81**	**1.24**	**3.26**	**3.74**	**0.57**	**1.51**
	4752-4755	1.45	1.02	0.30	0.82	1.22	2.51	1.99	0.67	1.51
	4851-4854	1.36	0.99	0.57	0.79	1.27	4.73	2.48	0.45	2.07
	4923-4926	1.45	1.04	0.62	0.84	1.20	2.76	4.12	0.88	1.60
	4998-5001	1.38	1.00	0.67	0.82	1.22	2.98	3.05	0.74	1.69
Nerar Char (Sundarbans)	0-1 (cm)	0.23	0.82	1.76	0.30	3.36	1.66	0.69	0.08	8.63
	1-2 (cm)	0.51	0.78	0.69	0.64	1.57	0.47	0.28	0.42	0.67
	5-6 (cm)	0.43	1.65	1.13	0.54	1.84	0.48	0.31	0.38	0.83
	10-12 (cm)	0.22	0.30	0.47	0.67	1.50	0.40	0.30	0.17	1.70
Ashokanagar crude oil (Aliphatic)		1.08	1.07	0.06	0.85	1.17	1.92	0.71	0.43	1.40

CPI-1=½×(((
$C_{25}+C_{27}+C_{29}+C_{31}+C_{33}$)/ ($C_{24}+C_{26}+C_{28}+C_{30}+C_{32}$)) +
(($C_{25}+C_{27}+C_{29}+C_{31}+C_{33}$/($C_{26}+C_{28}+C_{30}+C_{32}+C_{34}$)))
CPI-2 =½×(((
$C_{25}+C_{27}+C_{29}+C_{31}$) + ($C_{27}+C_{29}+C_{31}+C_{33}$))/ ($C_{26}+C_{28}+C_{30}+C_{32}$))
P_{aq} = ($C_{23}+C_{25}$)/ ($C_{23}+C_{25}+C_{29}+C_{31}$)
Inverse P_{aq} =1/P_{aq}; Pristane/Phytane ratio = Pr/Ph
TAR = ($C_{27}+C_{29}+C_{31}$)/ ($C_{15}+C_{17}+C_{19}$)

Table 6. Geochemical and maturity proxies of Ashoknagar crude oil.

Sample Id	API°	Pr/Ph	DMNr	TMNr	TeMNr	PMNr	DBT/Phe	MDR	MPI	VRC%	VRM%
Crude oil	41	6.20	0.65	0.28	0.66	0.35	0.10	1.99	0.36	0.61	0.66

API, API Gravity; Pr/Ph, Pristane/Phytane; DBT, Dibenzothiophene; Phe-Phenanthrene; MDR, 4-MDBT/1-MDBT; MDBT, Methyldibenzothiophene; TMNr, 1,3,7-/1,3,7- + 1,2,5-TMN (trimethylnaphthalene ratio); TeMNr, 1,3,6,7-/1,3,6,7- + (1,2,5,6-+1,2,3,5-)TeMN; PMNr , 1,2,4,6-/1,2,4,6- + 1,2,3,5-PMN; MPI, Methylphenanthrene Index = {1.5 _ ([2-MP] + [3-MP])/(Phenanthrene+ [1-MP]+ [9-MP])}, where MP-Methylphenanthrene; VRc, 0.60 _ MPI + 0.40; VRm = 0.073 _ MDR + 0.51.

Discussion

Stable isotope source signature of OM and its depositional environment

The C/N ratio of the shale samples, indicating mixed freshwater algae (C/N ratio 6-8) and terrestrial plants (C/N > 15) derived OM source (Meyers, 1994). An increase in the C/N ratio with depth is likely mediated by an increase in TOC values instead of selective removal of N and indicates a change in OM source from freshwater phytoplankton during Pliocene and Pleistocene to C_3 plants growing in marshy depositional settings during Miocene (Fig. 2b). The $\delta^{13}C$ composition coupled with the C/N ratio is further used to delineate the sources of OM, especially to identify the relative contribution from aquatic versus terrestrial sources (Das et al., 2008; Ramaswamy et al., 2008; Cai et al., 2015; Careddu et al., 2015; Li et al., 2016). The $\delta^{13}C$ vs C/N plot (Fig. 3b) of the studied samples indicates a primarily freshwater phytoplankton and C_3 terrestrial plant/ freshwater macroalgal source of OM (Cerling and Harris, 1999; Diefendorf et al., 2010; Kohn, 2010; Cernusak et al., 2013). The presence of Type III kerogen in these samples is consistent with our observation because kerogen type does not discriminate between terrestrial higher plant and freshwater aquatic plant-derived sources of OM. Our observation matches with the reported presence of terrestrial (humic) OM in the Bengal Basin (Bengal Foredeep) sediments as described by Shamsuddin and Khan (1991), who used the $\delta^{13}C$ composition of hydrocarbon gases to postulate the source of the sedimentary OM. The $\delta^{13}C$ vs C/N plot may also indicate specific depositional environments such as tidal flats, C_3 marsh and brackish transition zones (Khan et al., 2015). The studied samples mostly fall in the tidal flat and C_3 marsh zone, as indicated by the $\delta^{13}C$ vs C/N plot (Fig. 3a). A gradual change in the OM source from aquatic (Pleisto-Pliocene) to terrestrial C_3 plant (Miocene) and from tidal flat (Pleisto-Pliocene) to C_3 marsh (Miocene) depositional environments with age is also evident in the $\delta^{13}C$ vs C/N plots. The absence of C_4 plant-derived OM in the studied Bengal Basin sediments, despite the reported presence of C_4 plants in the Lower Ganga Plain (Basu et al., 2015), may result from the low preservation potential of OM derived from the C_4 plants (Wynn and Bird, 2007). Two Well C-1 samples having depth intervals of 860-865 m and 960-965 m show slightly more enriched $\delta^{13}C$ values (-21.8‰ and -21.7‰, respectively), indicating a blend of C_3 and C_4 plant-derived OM (Fig. 2. a & b).

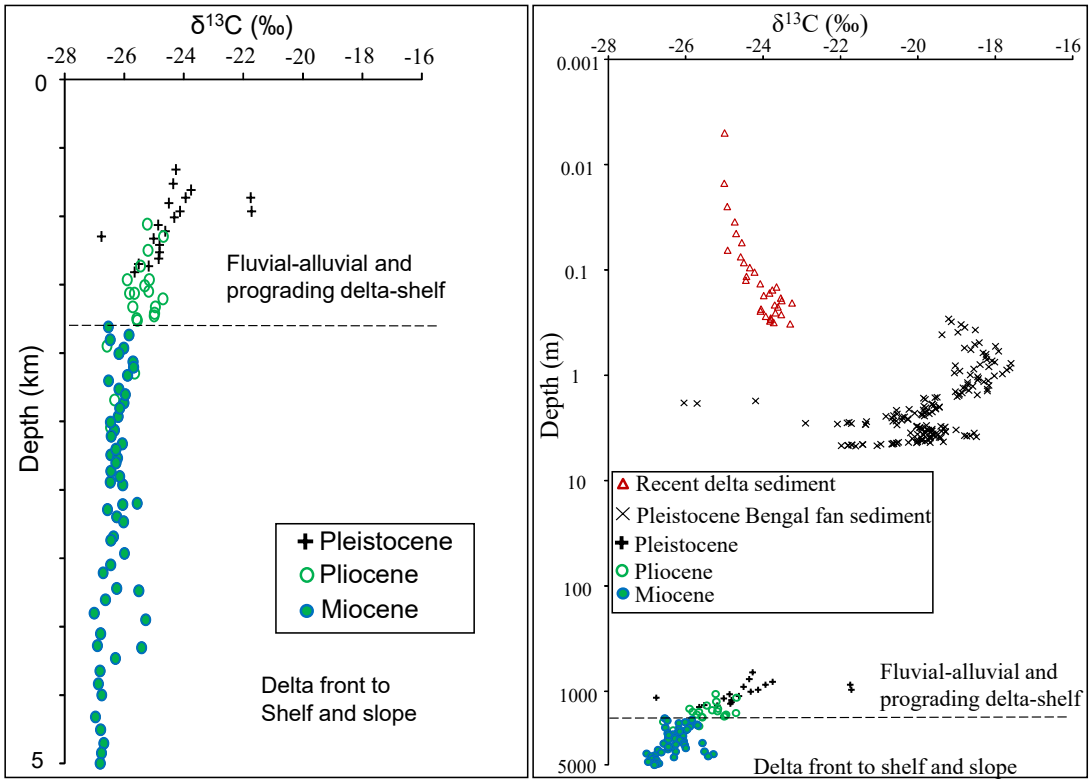

Fig. 2. (a) $\delta^{13}C$ vs depth plot of shale and sediment samples.

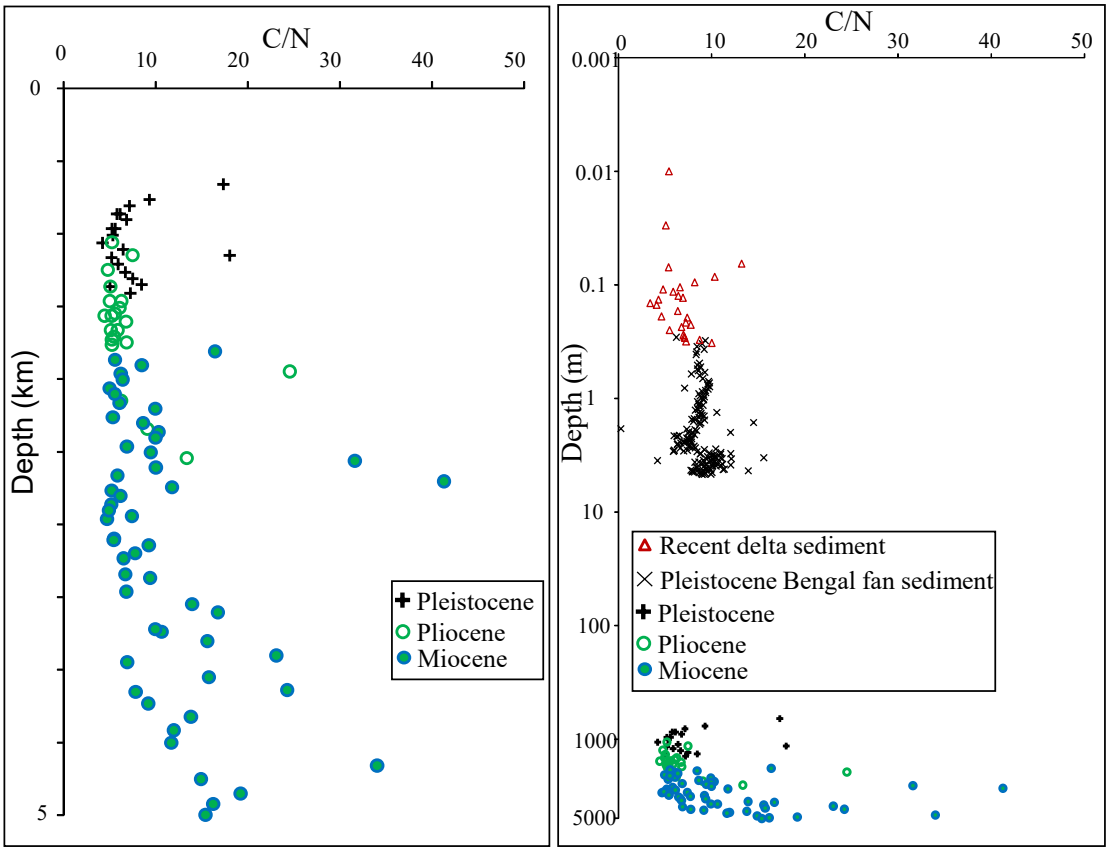

Fig. 2. b. C/N vs depth plot of shale and sediment samples.

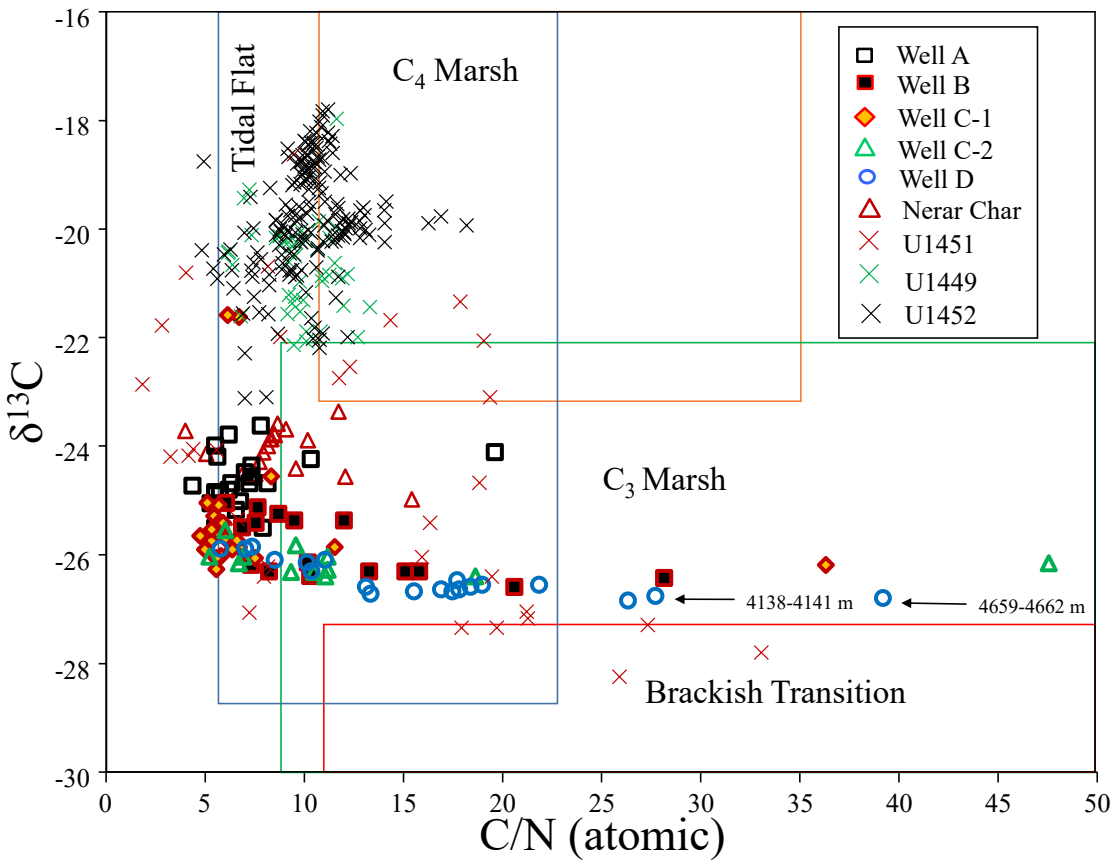

Fig. 3a. $\delta^{13}C$ vs C/N plot of shale and sediment samples.

More enriched $\delta^{13}C$ values in Pleistocene sediments of the Bengal Basin are consistent with the reported presence of C_4 plant-derived OM in Bengal Fan sediments although the reported appearance of C_4 plant-derived OM has been noticed in lower Bengal Fan sediments since the Miocene (France-Lanord and Derry, 1994; Galy et al., 2010). The absence of a mixed C_3-C_4 signal in Miocene Bengal Basin sediments may further be explained in light of the possible lower abundance of C_4 plants in marginal marine environments. Early diagenesis and post-depositional decomposition of OM primarily affect the C/N ratio (e.g., Walker and McComb, 1985). The stable isotope signature is considered resistant to isotopic alteration during post-depositional diagenesis (Schelske and Hodell, 1995; Teranes and Bernasconi, 2000; Kemp et al., 2012), although selective preservation of ^{13}C-depleted compounds under oxic environments (Lehmann et al., 2002) and ^{15}N enrichment in residual OM is reported (Middelburg and Herman, 2007). The influence of decomposition on the $\delta^{13}C$ value depends on the type of OM, whereas the effect on $\delta^{15}N$ is primarily microbially controlled (Galman et al., 2009). In the studied Bengal Basin sediments, an insignificant correlation ($R^2 < 0.4$) between C/N and $\delta^{13}C$ (except Well D) and between C/N and $\delta^{15}N$ ($R^2 < 0.3$) indicates that the stable isotope signature

of the sedimentary OM is not significantly affected by bacterial decomposition (Fig. 4. a, b). Significant correlation (R^2 = 0.6) between C/N and $\delta^{15}N$ likely indicates C_3 marsh source of OM. The $\delta^{15}N$ signature of C_3 marsh plants, such as mangroves, is generally higher than terrestrial plants (Kuramoto and Minagawa, 2001). Selective loss of ^{14}N through denitrification, occurring at the sediment-water interface, and selective removal of diagenetically sensitive amino acids under oxic conditions (Nguyen and Harvey, 1997; M¨obius et al., 2010) may further contribute to the heavier $\delta^{15}N$ values (Natelhoffer and Fry, 1988; H¨ogberg, 1990; Kuramoto and Minagawa, 2001; Bedard-Haughn et al., 2003).

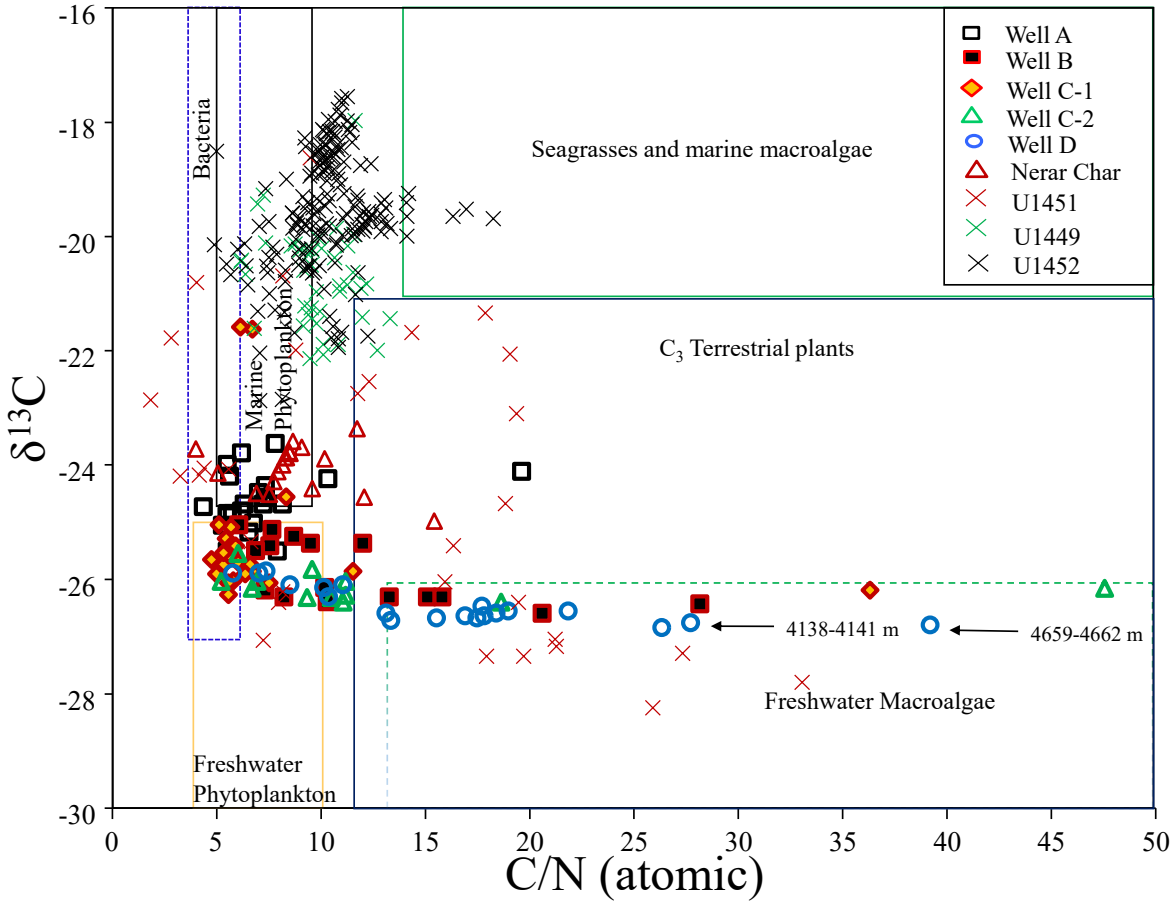

Fig. 3b. $\delta^{13}C$ vs C/N plot of shale and sediment samples.

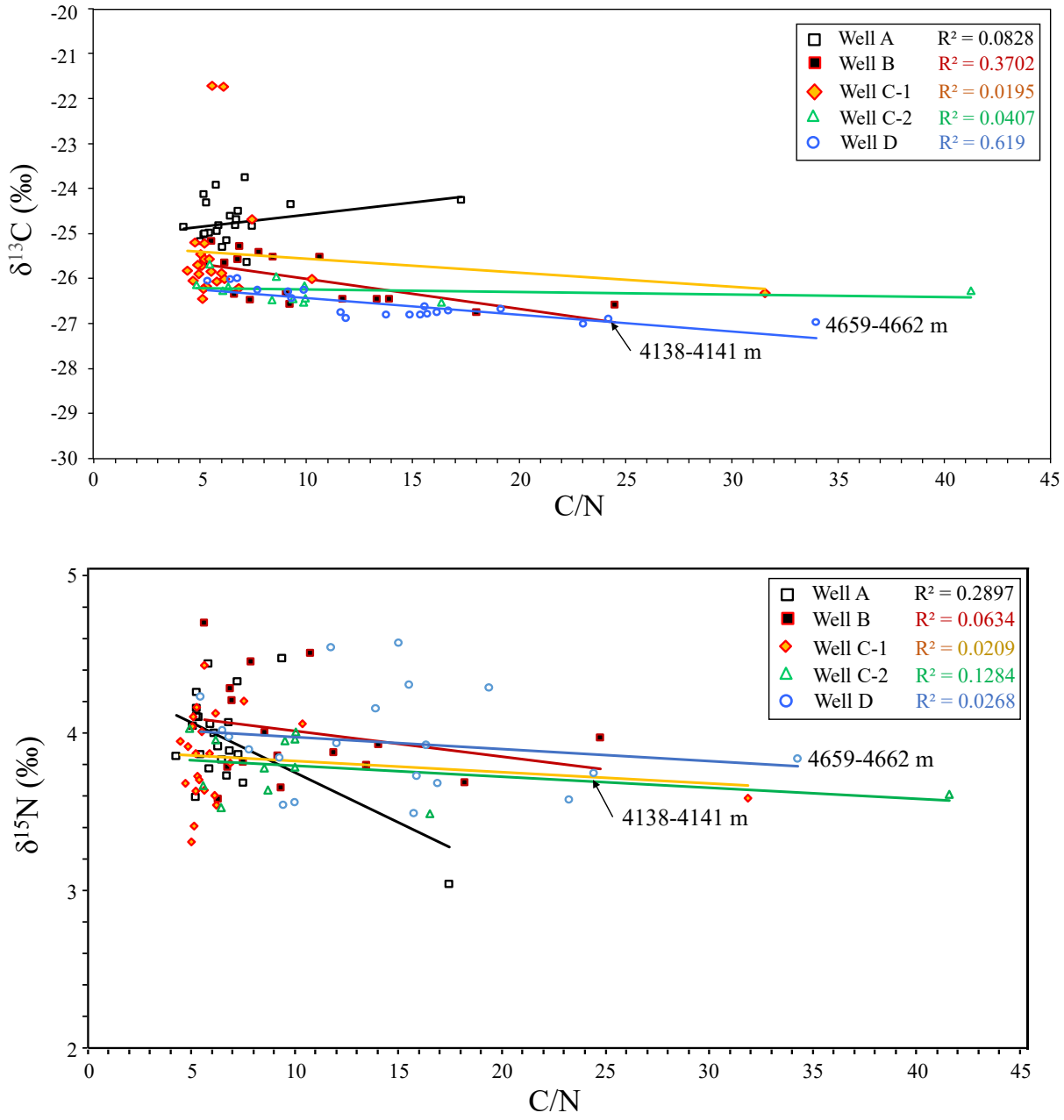

Fig. 4. (a) $\delta^{15}N$ vs C/N and (b) $\delta^{13}C$ vs C/N plot.

I do not observe a systematic change in $\delta^{15}N$ values with depth, although an increase in $\delta^{15}N$ values due to microbial decomposition with depth is often observed (Billings and Richter, 2006; Craine et al., 2015). This may not imply an absence of diagenetic effects, but rather that the sedimentary OM is mostly resistant to further degradation and less sensitive to post-depositional diagenetic changes.

Source and depositional environment interpretation using alkane distribution

The GC-MS analysis shows the presence of *n*-alkanes (*n*-C_{14-35}) and isoprenoid alkanes (pristane and phytane) in samples from Well B, Well C-1, Well C-2, Well D, and Nerar Char. Crude oil shows *n*-alkanes (*n*-C_{11-34}) with maxima peak at *n*-$C_{15.}$ Phytoplankton and algae primarily produce short-chain *n*-alkanes (*n*-C_{14} to *n*-C_{24}), enriched in *n*-$C_{15, 17, 19}$ with dominant *n*-C_{17} alkane, and show a strong odd over even carbon preference (Meyers and Ishiwatari, 1993; Meyers, 1997; Sakata et al., 1997; Meyers and Teranes, 2001). Microbial activity (as well as fossil fuel input) contributes to the short-chain *n*-alkanes without any strong odd over even carbon number preference (Bouloubassi et al., 1998). Terrestrial higher (vascular) plants produce long-chain *n*-alkanes (*n*-C_{25} to *n*-C_{35}) enriched in *n*- $C_{27, 29, 31}$ alkanes with a strong odd-to-even carbon preference (Eglinton and Hamilton, 1967). In some instances, long-chain *n*-alkanes are linked to phytoplankton and microbial sources, but an odd over-even carbon preference is not observed (Volkman et al., 1998). Aquatic plants, including floating and submerged species, are characterised by *n*- $C_{21, 23, 25}$ alkanes (Meyers and Teranes, 2001). The CPI takes into account the relative abundance of odd vs even *n*-alkanes and indicates the source of the immature sedimentary OM (Bush and McInerney, 2013). Terrestrial higher plants typically show high (> 5) CPI-2 (CPI_{25-35}) values with strong odd-to-even carbon preference (Eglinton and Hamilton, 1967; Rieley et al., 1991; Bouloubassi et al., 1998). On the contrary, phytoplankton and aquatic plant-derived OM exhibit CPI-1 ($CPI1_{5-19}$) values close to unity (Tareq et al., 2005; Jeng, 2006). Long-chain *n*-alkanes derived from marine phytoplankton, microorganisms and hydrocarbon generally do not have an odd-to-even carbon preference (Volkman et al., 1998). Near-unity CPI-1 (1.0-1.6) and CPI-2 (0.8-1.0) values in shale samples indicate the absence of strong odd-even carbon preference and primarily an aquatic source of OM. The sediment samples show both CPI-1 and CPI-2 values below the unity. CPI values close to 1.0 may also result from microbial activity or thermal alteration of kerogen (Xing et al., 2011). The measurable presence of methanogenic archaea only in two Miocene sediments (discussed below) does not support extensive microbial activity. Instead, a geothermal gradient of ~27-28 ºC km^{-1} in Bengal Basin (Akbar 2011) implies the onset of thermal maturity of deeper Miocene sediments. Our observation is supported by terrigenous to aquatic ratio (TAR) values < 1 (Table 5) of the studied samples (Bourbonniere and Meyers, 1996; Silliman et al., 1996; Ortiz et al., 2013). An increase in TAR values with depth indicates a change in the source of OM from aquatic (during Pliocene and Pleistocene) to terrestrial (Miocene).

The Paq is used to determine the relative contribution of terrestrial plants (Paq < 0.1), emergent aquatic plants (Paq = 0.1-0.4) and non-emergent (submerged and floating) aquatic plants (Paq = 0.4-1.0) to the sedimentary OM (Ficken et al., 2000). The Paq (0.8-0.9) values of the studied shale samples (Table 5) indicate a primarily non-emergent aquatic plant source of the sedimentary OM. Sediment samples show Paq values (0.3-0.7), suggesting a non-emergent aquatic plant source of OM, but recent sediment shows elevated Paq due to a lack of diagenetic effect. Our interpretation based on the CPI, TAR, and Paq values is consistent with the source interpretation based on the Rock-Eval pyrolysis, elemental C/N ratio and stable isotope data.

Pristane (Pr) and phytane (Ph) are diagenetic products formed by oxidation and reduction of phytol, the side chain of chlorophyll-*a*. The Pr/Ph ratio is used to determine the source of OM and paleodepositional and palaeo-redox interpretations (Didyk et al., 1978; Peters et al., 2005). High (> 3.0) Pr/Ph ratio in rock samples indicates terrigenous plant-derived OM input and deposition under oxic conditions, whereas a low (< 0.8) Pr/Ph ratio indicates anoxic, mostly saline to hypersaline, paleodepositional conditions associated with evaporites and carbonates (Peters et al., 2005). Lower than unity Pr/Ph values (Table 5) in the Well B, Well C-1, Well C-2 and Nerar Char (except one) samples and relatively low Pr/Ph ratio (mostly 1-3) in the Well D samples indicate non-terrestrial OM source and suggest deposition under variable, anoxic to oxic conditions. The crude oil Pr/Ph (1.9) ratio indicates the source rock has a mixed source of OM. Notably, ten Haven et al. (1987) have advised against drawing conclusions on the paleoredox depositional conditions solely from the Pr/Ph ratio and assigned a low Pr/Ph ratio (< 1) to hypersaline environments. In line with this, Peters et al. (2005) do not recommend Pr/Ph ratios in the range of 0.8-3.0 for interpreting paleoenvironmental conditions without corroborating data. Hence, we use the Pr/*n*-C_{17} vs Ph/*n*-C_{18} cross plot for paleodepositional interpretation (Lijmbach, 1975). An oxic and terrestrial depositional settings are postulated from the Pr/*n*-C_{17} vs Ph/*n*-C_{18} cross plot (Fig. 5), except for one of the samples from the Well D and Nerar Char, samples from the Well C-1, Well C-2, crude oil that falls in the suboxic zone of deposition (Fig. 5). Two samples from Nerara Char fall under anoxic zone. Our observation is consistent with the reported immature nature of OM, postulated from higher Pr/*n*-C_{17} (2.7-5.6) and Pr/Ph ratios of the hydrocarbons (condensates) in the Bengal Foredeep region in Bangladesh (Shamsuddin and Khan, 1991). The Pr/*n*-C_{17} and Ph/*n*-C_{18} ratios (Peters et al., 1995, 1999) further indicate the degree of biodegradation of the OM. The Pr/*n*-C_{17} and Ph/*n*- C_{18} ratios increase with an increased microbial decomposition of OM during biodegradation due to the selective loss of *n*-alkanes compared to the isoprenoid alkanes (Peters

et al., 1999). We use the (Pr + *n*-C_{17})/(Ph + *n*-C_{18}) ratio to study biodegradation because the effect of variation of any one variable is less on the ratio (Alexander et al., 1981; Das et al., 2009). Above or near unity (Pr + *n*-C_{17})/(Ph + *n*-C_{18}) ratio values indicate biodegradation in deeper Miocene sediments from Well D, including intervals (4138-4141 m and 4659-4662 m), which show the presence of methanogenic archaea (discussed below). Samples at these depths were likely thermally altered (considering a geothermal gradient of 27.6 $^{\circ}$C km^{-1}). The use of (Pr + *n*-C_{17})/(Ph + *n*-C_{18}) ratio was based on the assumption that the isoprenoids result from degradation of the phytol side-chain of chlorophyll-*a*. However, pristane and phytane could be derived from thermally altered sedimentary OM containing isoprenoid components of archaeal lipids (Li et al., 1995; Rontani and Bonin, 2011). It is possible that the biodegradation reflected by the (Pr + *n*-C_{17})/(Ph + *n*-C_{18}) ratio was influenced by the isoprenoids released from the archaeal lipids during catagenesis.

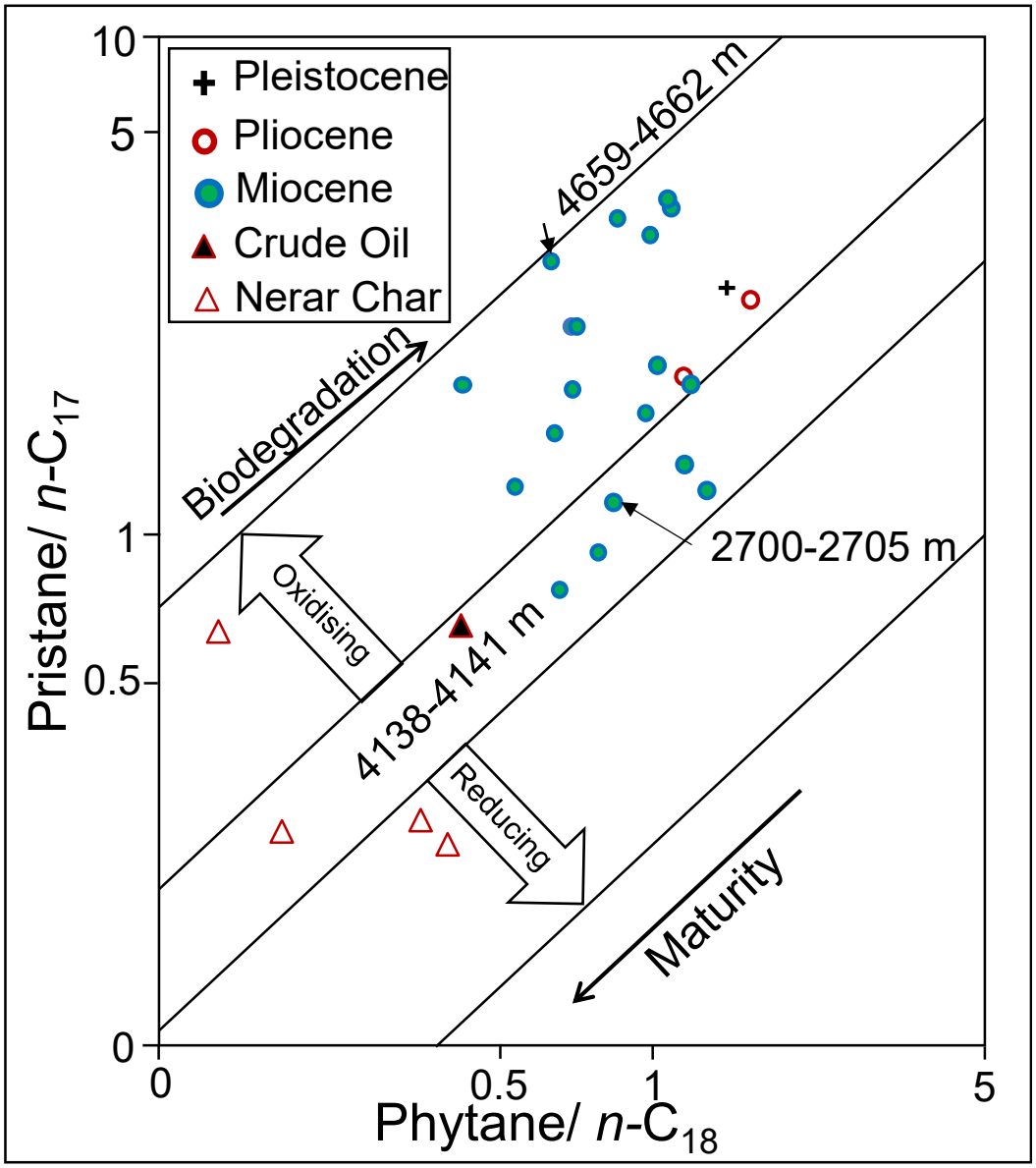

Fig. 5. Phytane/*n*-C_{18} vs pristane/*n*-C_{17} cross-plot.

Source and depositional environment interpretation using PAH distribution in crude oil

Several PAH compounds have been identified from Ashoknagar crude oil used for different biomarker proxies (Table. 6). The DBT/Phe ratio used to interpret the source rock lithology, the carbonate has values more than unity, whereas the shale has a value less than unity. The DBT/Phe ratio (0.1) indicates crude oil derived from source rock shale (Sivan et al., 2008). The DBT vs Pr/Ph ratio plot indicates the source rock of marine shale/lacustrine depositional environment (Fig. 6).

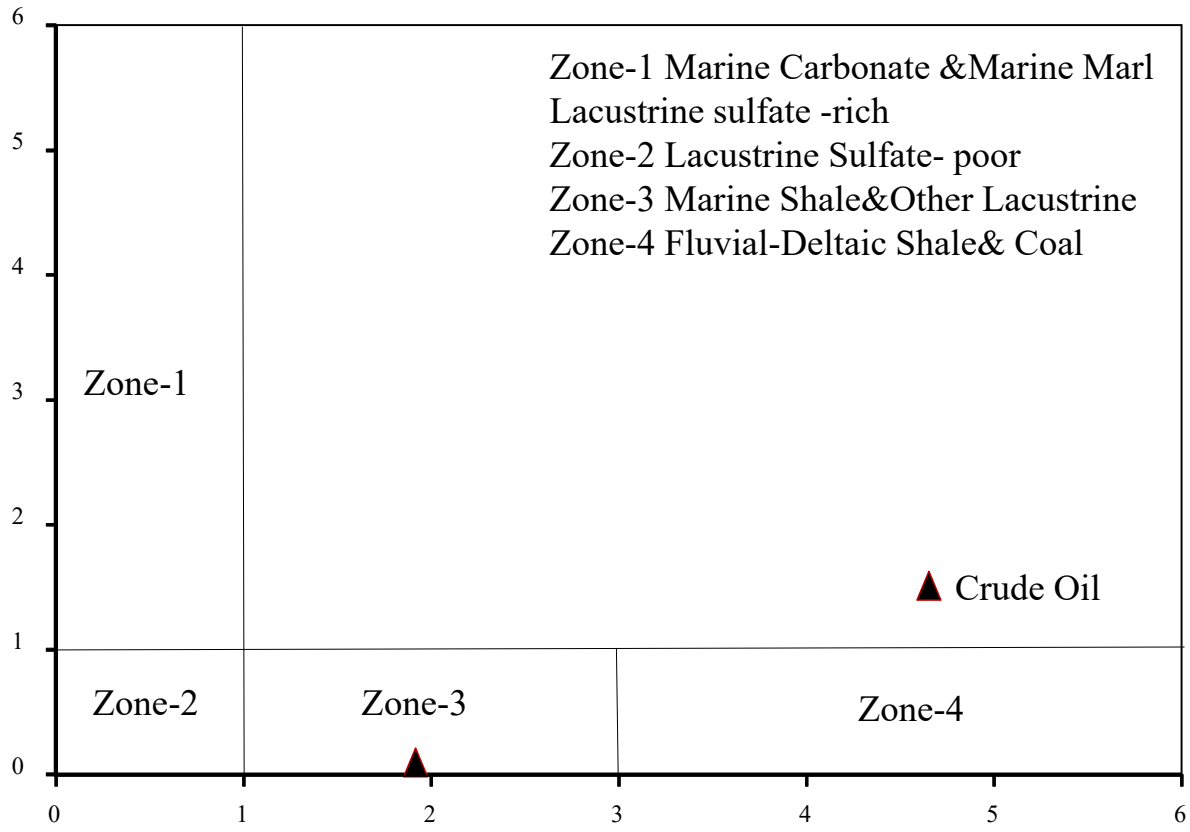

Fig. 6. DBT/Phenathrene vs Pr/Ph plot.

Phylogenetic diversity of methanogens

The studied samples do not show the presence of sulfur oxidising and sulphate-reducing prokaryotes. A low diversity of methanogenic archaea was detected, and two dominant genera, *Methanocella* sp. and *Methanoformis* sp., are found in Well D (4138-4141 m and 4659-4662 m) samples (Fig. 5). The presence of methanogenic archaea indicates active biogenic methane generation at these depths in Well D (4138-4141 m and 4659-4662 m). Methanogenic archaea (*Methanocella* sp. and *Methanoformis* sp.) reported in the two Well D samples belong to hyperthermophilic groups (Mauerhofer et al., 2021) and could thrive well within the temperature ranges estimated from an average geothermal gradient of 27.6 ◦C km^{-1} in the Bengal Basin (Akbar, 2011). The non-detection of prokaryotic methanogenesis gene signatures in the rest of the samples could possibly result from an absence of labile OM and/or unfavourable substrate conditions. Interestingly, the OM source of the two Well D samples, which show the presence of methanogenic archaea, is C_3 freshwater macroalgae deposited under C_3 marshy conditions. Freshwater algae are associated with aliphatic and peptide-like labile compounds that may facilitate active methanogenesis (del Giorgio and Davis, 2003; Kellerman et al., 2018; Berberich et al., 2020). Enhanced methane production has been

observed in OM derived from aquatic plants (Yakimovich et al., 2018), and experimental studies show higher methanogenic activities in sediments containing freshwater OM (Berberich et al., 2020; Yakimovich et al., 2020), although little published literature, exploring the effects of OM type on methanogens, exists.

FT-IR Spectroscopy derived source rock maturity

FTIR spectroscopy was used to evaluate the structural characterisation of the asphaltene, maltene and whole oil. The ^{1}H and ^{13}C NMR spectroscopy was performed on asphaltene for functional group cross-verification with FTIR data. The asphaltene reflects the characteristics of the source rock (Asemani and Rabbani, 2016). The C-factor ($C{=}CC{=}C{+}C{=}O$) of the asphaltene varies between unity and near zero and decreases with the increase in maturity of the source rock (Ganz and Kalkreuth, 1987; Kister et al., 1990). A measured C-factor value of 0.5 of the studied asphaltene fraction of Ashoknagar crude oil indicates the source rock is not over-matured. However, the low C-factor values (0.2) of the whole crude indicate the mature nature of the oil. The FITR parameters, such as the aliphatic index (0.8 and 0.6), are higher than the aromatic index (0.1) in both the crude and asphaltene. Oxygenated functional groups enriched in asphaltene (0.3) compared to crude oil (0.1).

Organic matter source, maturity and hydrocarbon potential of Bengal Basin sediments

TOC values > 1% in seven out of 93 samples fall in the fair hydrocarbon sources field in the HI/TOC plot (Fig. 7). With an average geothermal gradient of 27.6 ˚C km^{-1} (Akbar, 2011), it is likely that the deeper samples of these wells have reached the catagenesis phase and are likely to reflect cracking processes, but the shallower samples lie close to the diagenesis-catagenesis boundary and are unlikely to show any effect of thermal alteration. Low Tmax values (297-303 ˚C) indicate immature kerogen and insignificant hydrocarbon generation from these samples. The rest of the samples lie in the poor source sector of the HI/TOC plot (Fig. 7).

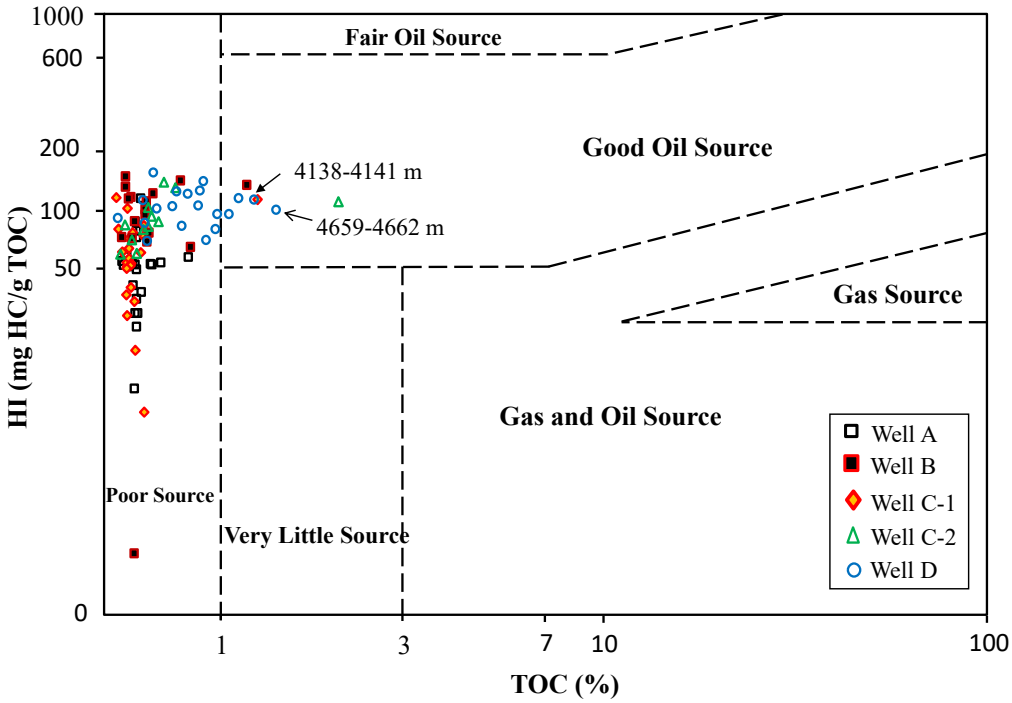

Fig. 7. Hydrogen index vs TOC of shale samples

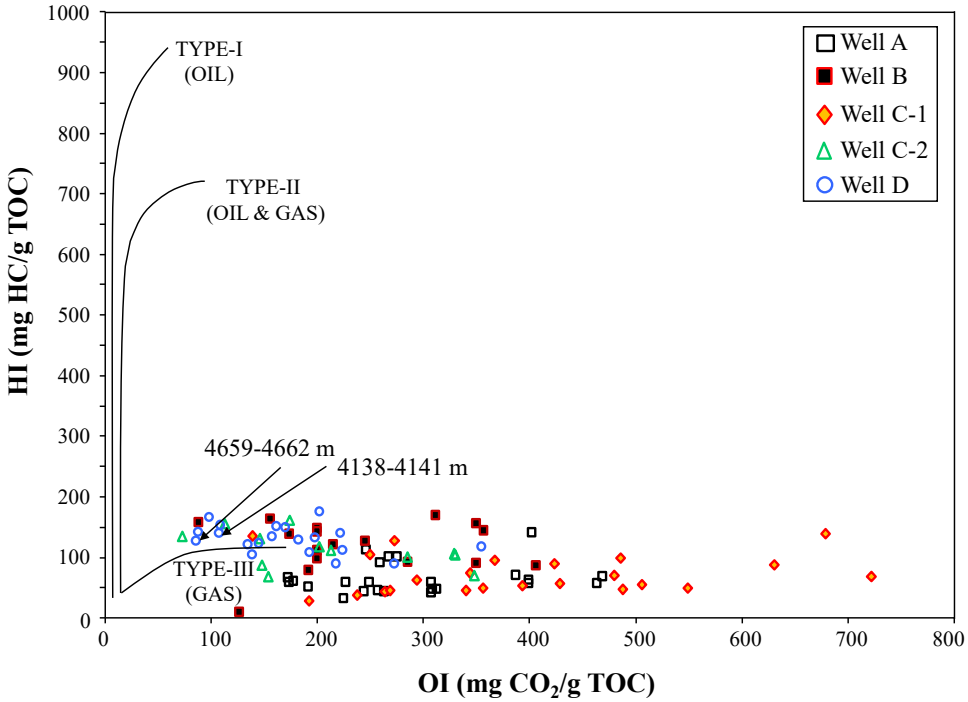

Fig. 8a. Hydrogen index vs oxygen index plot of shale samples.

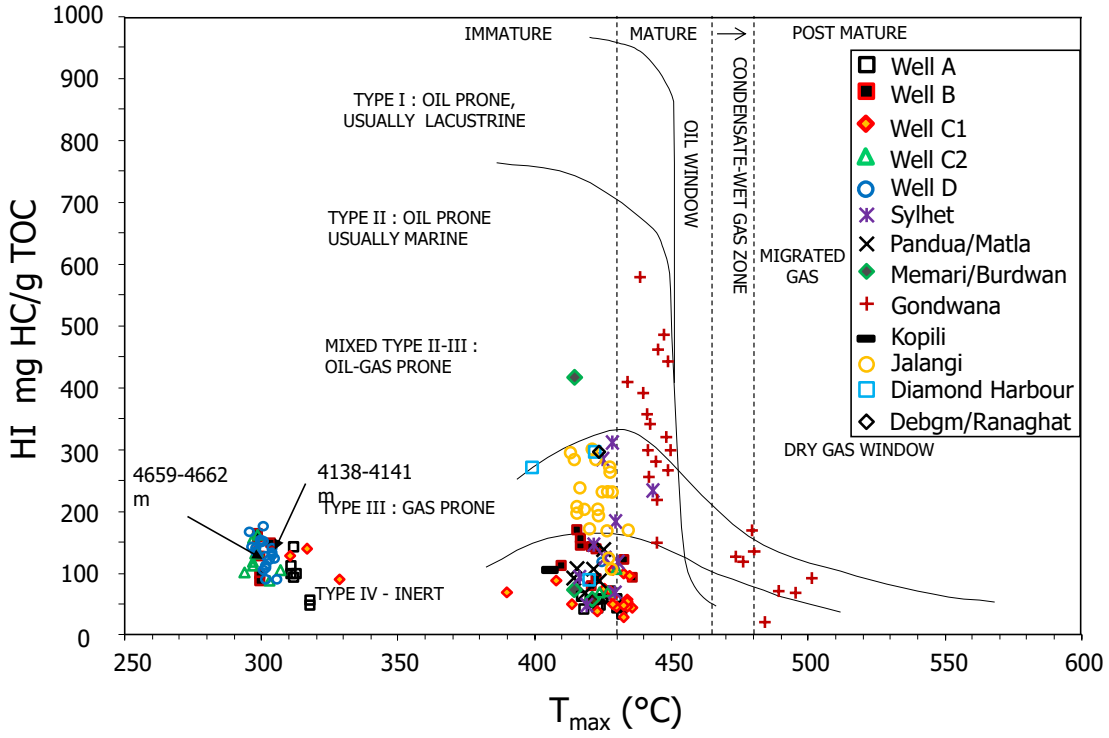

Fig. 8b. Hydrogen index vs Tmax plot of shale samples.

The kerogen type provides information about the origin, diagenesis and maturity of OM (e.g., Peters, 1986; Boreham and Powell, 1993; Littke and Leythaeuser, 1993). The HI/OI plot (Fig. 8a) indicates the presence of Type III (gas-prone) kerogen in the studied samples (Tissot and Welte, 1984; Laier et al., 1992). The Type III kerogen indicates terrestrial OM source. The HI/Tmax plot (Fig. 8b) indicates the mostly immature nature of the samples, and the plot is consistent with the presence of Type III and Type IV kerogen in the samples. Those samples with TOC > 1% fall within the immature Type III kerogen zone in Fig. 8b. Similarly, the presence of Type III containing immature OM (TOC = 0.2-0.6%) is reported in the Miocene Bengal Basin (Foredeep) sediments in Bangladesh (Shamsuddin and Khan, 1991).

Crude oils from terrigenous OM sources show a lighter $\delta^{13}C$ signature than the marine source (Craig, 1953; Silverman, 1965; Ogbesejana et al., 2021). The $\delta^{13}C$ values (-28‰ to -23.5‰) of low sulfur (<0.5%) rich oils indicate the marine deltaic source (Chung et al., 1992). The oil generated from carbonate source rocks shows a lighter $\delta^{13}C$ and heavier $\delta^{2}H$ signature than the shale-sourced oils (Barrie et al., 2018). Furthermore, the $\delta^{13}C$ signature of oil becomes heavier with increasing maturation (Clayton, 1991). The $\delta^{13}C$ value of Ashoknagar crude (24.8‰) falls within the $\delta^{13}C$ range of marine sourced oil (-24‰ to -27‰) and is heavier than

the $\delta^{13}C$ values of non-marine oil (-30‰ to -32‰) (Table 7). The low TS content (0.03%) of the Ashoknagar oil indicates a marine deltaic source.

Table 7. $\delta^{13}C$ and $\delta^{2}H$ isotope ratio of published marine and non-marine oils.

	Area	$\delta^{13}C$ (‰)	$\delta^{2}H$ (‰)	References
Marine Oil	Gulf of Mexico, offshore	-26.5 ± 0.7	-	Chung et al., 1992
		-26.9 ± 0.6	-	
	Gulf of Mexico, onshore	-25.7 ± 1.0	-	
		-24.8 ± 0.6	-	
	Scotian basin	-25.6 ± 0.1	-	
	Avalon basin	-25.6 ± 0.1	-	
	North Slope, Alaska	-29.6 ± 0.4	-	
		-30.4 ± 0.4	-	
	California	-22.8 ± 0.4	-	
	Choctaw, AL	-25.0	-85	
	Mobile, AL	-23. 3	-88	
	Cook Inlet, AK	-28. 7 to -30.4	-132 to -137	
	N. Cook Inlet, AK	-30.5	-130	
	Swanson River, AK	-30. 7	-133	
	North Slope, AK	-29. 9	-132	
	Kenai, AK	-27.9	-252	
	Kern, CA	-26.5	-132	
	San Joaquin, CA	-29. 7	-153	
	Los Angeles, CA	-23.8	-132	
	Ventura. CA	-23. 1	-123	
	San Miguel, CO	-28.8	- 92	
	Fremont, CO	-28.9	-144	
	Washington, CO	-27. 3	-144	
	Hendry, FL	-27. 4	-103	
	Hamilton, IL	-29.5	-119	
	Bridgeport, IL	-30.4	-125	
	Crude oil-Duchesne field Utah	-30 to -31	-144	
Non-Marine Oil	Crude ail-Red Wash field, Utah	-31.0	-	Silverman et al., 1958
	Crude oil-Brennan Bottom field, Utah	-30.6	-	
	Crude oil-Flat Mesa field, Utah	-31.7	-	
	Uinta, UT	-31 to -32	-149 to -163	
	Duchesne, UT	-30 to -32	-141 to -156	

*AL- Alabama, AK- Alaska, CA- California, CO- Colorado, FL- Florida, IL- Illinois and UT-Utah.

Table 8. $\delta^{34}S$ isotope ratio of published marine and non-marine oils.

	Area	$\delta^{34}S$ (‰)	References
Marine Oil	Alabama and Mississippi (onshore)	-12.5 to 14.7	Wei et al. (2012)
Non-marine Oil	Uinta Middle Green River	28.2	Thode H. G. (1958)

The hydrogen stable isotope ratio is used for establishing oil-oil co-relationships and source rock evaluation, although hydrogen isotope exchange with surrounding environments during diagenetic and catagenetic processes influences the $\delta^{2}H$ signature of oil. The hydrocarbon fraction shows a heavier $\delta^{2}H$ signature due to thermal maturation (Ogbesejana et

al., 2021). Further, the δ^2H values of marine and non-marine source-derived oil show a range of -85‰ to -252‰ and -141‰ to -163‰, respectively (Table 7). The δ^2H value of Ashoknagar crude (-110‰) falls within the δ^2H signature of the marine sourced oil. The $\delta^{34}S$ values of marine sourced crude oil vary between -12.5‰ to 14.7‰, whereas the $\delta^{34}S$ value of non-marine crude oil is 25‰ (Table 8). The Ashoknagar crude oil $\delta^{34}S$ value falls in the marine crude oil range.

Conclusion

The C/N and stable isotope ratios indicate primarily aquatic and C_3 plant sources of the OM, and sediment deposition under tidal flat and marshy environments. The *n*-alkane distribution (CPI, TAR and Paq) in the studied samples agrees with the aquatic and C_3 terrestrial plant sources of the OM. A gradual change in the dominant OM source and depositional environments from Recent-Pliocene (aquatic; tidal flat) to Miocene (terrestrial C_3 plant; marsh) is evidenced in the $\delta^{13}C$ vs C/N plots and TAR values. Isoprenoid alkane distribution (Pr/Ph, Pr/*n*-C_{17} vs Ph/*n*-C_{18}) is consistent with a primarily non-marine aquatic plant source of the OM and indicates a terrestrial oxic depositional environment. Except for a few sediment samples and crude oil show sub-oxic to anoxic depositional environment. Kerogen maturity parameters, including Tmax, HI, OI and TOC, indicate an immature nature of the sedimentary OM. The HI/OI and HI/ Tmax plots indicate the presence of primarily Type III (gas-prone) and Type IV (inert) kerogen in the samples. The Miocene Well D sediments with aquatic macroalgae-derived immature Type III kerogen and deposited under a C_3 marshy environment shows the presence of methanogenic archaea (*Methanocella* sp. and *Methanoformis* sp.) belong to hyperthermophilic groups and could contribute to the transformation of generated hydrocarbons into methane. The $\delta^{13}C$, δ^2H and $\delta^{34}S$ signatures of Ashoknagar crude indicate a deltaic source of the oil.

References

Akbar, M.A., 2011. An assessment of the geothermal potential of Bangladesh. Geothermal Training Programme, Orkustofnun, Iceland. Reports, Number 5.

Alam, M., 1989. Geology and depositional history of Cenozoic sediments of the Bengal Basin of Bangladesh. Palaeogeography Palaeoclimatology Palaeoecology 69, 125-139.

Alam, M.M., 1995. Tide-dominated sedimentation in the upper Tertiary succession of the sitapahar anticline, Bangladesh. In: Flemming, B.W., Bortholma, A. (Eds.), Tidal Signatures in Modern and Ancient Sediments, vol. 24. Special Publications of the International Association of Sedimentologists, pp. 329-341.

Alam, M., Alam, M.M., Curray, J.R., Chowdhury, M.L.R., Gani, MR, 2003. An overview of the sedimentary geology of the Bengal basin in relation to the regional tectonic framework and basin-fill history. Sedimentary Geology 155, 179-208.

Alexander, R., Kagi, R., Woodhouse, G.W., 1981. Geochemical correlation of Windalia oil and extracts of winning group (Cretaceous) potential source rocks, Barrow Subbasin, Western Australia. American Association of Petroleum Geologists Bulletin 65, 235-250.

Allison, M.A., 1998. Geologic framework and environmental status of the Ganges-Brahmaputra Delta. Journal of Coastal Research 14, 826-836.

Asemani, M. and Rabbani, A.R., 2016. Oil-oil correlation by FTIR spectroscopy of asphaltene samples. Geosciences Journal, 20, pp.273-283.

Babu, P.V.L.P.A., 1976. A review on the oil & gas prospects of the Bengal basin based on photogeomorphological studies. Journal of the Indian Society of Photo-Interpretation 4, 1-13.

Banerji, RK, 1984. Post-Eocene biofacies, palaeoenvironments and palaeogeography of the Bengal basin, India. Palaeogeography Palaeoclimatology Palaeoecology 45, 49-73.

Banerji, B., Ghosh, A., Pal, A.K., 1990. Eocene fossil algae from the subcrops of the Bengal Basin. Journal of the Palaeontological Society of India 35, 131-136.

Barrie, C.D., Taylor, K.W., Zumberge, J., 2018. A Multiple Isotope (C, H, S & O) Approach to Characterising Crude Oil Families Within Oil Basins. In American Association of Petroleum Geologists ACE.

Bastia, R., 2006. An overview of Indian sedimentary basins with special focus on emerging east coast deepwater frontiers. The Leading Edge 25, 818-829.

Basu, T.K., 1962. Subsurface Geology of the Indo-Stanvac concession, West Bengal. In: Proceedings of the Seminar on oil prospects in the Ganga Valley, Oil & Natural Gas Commission, Dehradun, pp. 25-27.

Basu, S., Argawal, S., Sanyal, P., Mahato, P., Kumar, S., Sarkar, A., 2015. Carbon isotopic ratios of modern C_3-C_4 plants from the Gangetic Plain, India and its implications to

paleovegetational reconstruction. Palaeogeography, Palaeoclimatology, Palaeoecology 440, 22-32.

Bedard-Haughn, A., van Groenigen, J.W., Van Kessel, C., 2003. Tracing 15N through landscapes: potential uses and precautions. Journal of Hydrology 272, 175-190.

Behar, F., Beaumont, V., Penteado, H.D.B., 2001. Rock-Eval 6 technology: performances and developments. Oil & Gas Science and Technology 56, 111-134.

Behera, P.K., Das, S.K., Ghosh, D., Mani, D., Kalpana, M.S., Ikehara, M., Patel, P.P., 2022. Organic biogeochemical study of deeper southeastern Bengal Basin sediments in West Bengal, India. Organic Geochemistry, p.104451.

Berberich, M.E., Beaulieu, J.J., Hamilton, T.L., Waldo, S., Buffam, I., 2020. Spatial variability of sediment methane production and methanogen communities within a eutrophic reservoir: Importance of organic matter source and quantity. Limnology and oceanography 65, 1336-1358.

Billings, S.A., Richter, D.D., 2006. Changes in stable isotopic signatures of soil nitrogen and carbon during 40 years of forest development. Oecologia 148, 325-333.

BOGMC, 1997. Petroleum exploration opportunities in Bangladesh. Bangladesh Oil, Gas and Mineral Corporation (Petrobangla), Dhaka.

Boreham, C.J., Powell, T.G., 1993. Petroleum source rock potential of coal and associated sediments: qualitative and quantitative aspects. In: Law, BE, Rice, DD. (Eds.), Hydrocarbons from Coal, American Association of Petroleum Geologists Studies in Geology, vol. 38, pp. 133-157.

Bouloubassi, I., Guehenneux, G., Rullk¨otter, J., 1998. Biological marker significance of organic matter in sapropels from the Mediterranean ridge, Site 969. In: Proceedings of the Ocean Drilling Program, Scientific Results, pp. 261-270.

Bourbonniere, R.A., Meyers, P.A., 1996. Sedimentary geolipid records of historical changes in the watersheds and productivities of Lakes Ontario and Erie. Limnology and Oceanography 41, 352-359.

Bush, R.T., McInerney, F.A., 2013. Leaf wax *n*-alkane distributions in and across modern plants: Implications for paleoecology and chemotaxonomy. Geochimica et Cosmochimica Acta 117, 161-179.

Cai, Y., Guo, L., Wang, X., Aiken, G., 2015. Abundance, stable isotopic composition, and export fluxes of DOC, POC, and DIC from the Lower Mississippi River during 2006-2008. Journal of Geophysical Research: Biogeosciences 120, 2273-2288.

Careddu, G., Costantini, M.L., Calizza, E., Carlino, P., Bentivoglio, F., Orlandi, L., Rossi, L., 2015. Effects of terrestrial input on macro benthic food webs of the coastal sea are detected by stable isotope analysis in Gaeta Gulf. Estuarine, Coastal and Shelf Science 154, 158-168.

Cerling, T.E., Harris, J.M., 1999. Carbon isotope fractionation between diet and bioapatite in ungulate mammals and implications for ecological and paleoecological studies. Oecologia 120, 347-363.

Cernusak, L.A., Ubierna, N., Winter, K., Holtum, J.A., Marshall, J.D., Farquhar, G.D., 2013. Environmental and physiological determinants of carbon isotope discrimination in terrestrial plants. New Phytologist 200, 950-965.

Chung, H.M., Rooney, M.A., Toon, M.B., Claypool, G.E., 1992. Carbon isotope composition of marine crude oils. American Association of Petroleum Geologists Bulletin 76, 1000-1007.

Clayton, C.J., 1991. Effect of maturity on carbon isotope ratios of oils and condensates. Organic Geochemistry, 17, 887-899.

Craig, H., 1953. The geochemistry of the stable carbon isotopes. Geochimica et cosmochimica acta, 3, 53-92.

Craine, J.M., Brookshire, E.N.J., Cramer, M.D., Hasselquist, N.J., Koba, K., Marin- Spiotta, E., Wang, L., 2015. Ecological interpretations of nitrogen isotope ratios of terrestrial plants and soils. Plant and Soil 396, 1-26.

Curray, J.R., 1991. Geological history of the Bengal geosyncline. Journal of Association of Exploration Geophysicists XII 209-219.

Curray, J.R., Munasinghe, T., 1991. Origin of the Rajmahal Traps and the 85jE Ridge: preliminary reconstructions of the trace of the Crozet hotspot. Geology 19, 1237-1240.

Das, S.K., Routh, J., Roychoudhury, A.N., Klump, J.V., 2008. Elemental (C, N, H, and P) and stable isotope ($\delta^{15}N$ and $\delta^{13}C$) signatures in sediments from Zeekoevlei, South Africa: a record of human intervention in the lake. Journal of Paleolimnology 39, 349-360.

Das, S.K., Routh, J., Roychoudhury, A.N., 2009. Biomarker evidence of macrophyte and plankton community changes in Zeekoevlei, a shallow lake in South Africa. Journal of Paleolimnology 41, 507-521.

del Giorgio, P.A., Davis, J., 2003. Patterns in dissolved organic matter lability and consumption across aquatic ecosystems. In: Aquatic ecosystems. Academic Press, pp. 399-424.

Didyk, B.M., Simoneit, B.R.T., Brassell, S.C., Eglinton, G., 1978. Organic geochemical indicators of palaeoenvironmental conditions of sedimentation. Nature 272, 216-222.

Diefendorf, A.F., Mueller, K.E., Wing, S.L., Koch, P.L., Freeman, K.H., 2010. Global patterns in leaf ^{13}C discrimination and implications for studies of past and future climate. Proceedings of the National Academy of Sciences of the United States of America 107, 5738-5743.

Directorate General of Hydrocarbon, 2019. India's hydrocarbon outlook, 2018-19, a report on exploration & production activites.

Eglinton, G., Hamilton, R.J., 1967. Leaf epicuticular waxes. Science 156, 1322-1335.

Ficken, K.J., Li, B., Swain, D.L., Eglinton, G., 2000. An *n*-alkane proxy for the sedimentary input of submerged/floating freshwater aquatic macrophytes. Organic Geochemistry 31, 745-749.

France-Lanord, C., Derry, L.A., 1994. $\delta^{13}C$ of organic carbon in the Bengal Fan: source evolution and transport of C_3 and C_4 plant carbon to marine sediments. Geochimica et Cosmochimica Acta 58, 4809-4814.

Galman, V., Rydberg, J., Bigler, C., 2009. Decadal diagenetic effects on $\delta^{13}C$ and $\delta^{15}N$ studied in varved lake sediment. Limnology and Oceanography 54, 917-924.

Galy, V., France-Lanord, C., Peucker-Ehrenbrinkm, B., Huyghem, P., 2010. Sr-Nd-Os evidence for a stable erosion regime in the Himalaya during the past 12 Myr. Earth and Planetary Science Letters 290, 474-480.

Ganz, H. and Kalkreuth, W., 1987. Application of infrared spectroscopy to the classification of kerogen types and the evaluation of source rock and oil shale potentials. Fuel, 66(5), pp.708-711.

H¨ogberg, P., 1990. Forests losing large quantities of nitrogen have elevated ^{15}N:^{14}N ratios. Oecologia 84, 229-231.

Hossain, M., Khan, M., Hossain, S., Chowdhury, K.R., Abdullah, R., 2019. Synthesis of the tectonic and structural elements of the Bengal Basin and its surroundings. In: Tectonics and Structural Geology: Indian Context. Springer, Cham, pp. 135-218.

Hossain, H.M.Z., Sampei, Y., Roser, B.P., 2009. Characterisation of organic matter and depositional environment of Tertiary mudstones from the Sylhet Basin, Bangladesh. Organic Geochemistry 40, 743-754.

Huber, T., Faulkner, G., Hugenholtz, P., 2004. Bellerophon: a program to detect chimeric sequences in multiple sequence alignments. Bioinformatics 20, 2317-2319.

Imam, B.I., Hussain, M., 2002. A review of hydrocarbon habitats in Bangladesh. Journal of Petroleum Geology 25, 31-52.

Islam, M.A., 2009. Diagenesis and reservoir quality of Bhuban sandstones (Neogene), Titas Gas Field, Bengal Basin, Bangladesh. Journal of Asian Earth Sciences 35, 89-100.

Jeng, W.-L., 2006. Higher plant *n*-alkanes average chain length as an indicator of petrogenic hydrocarbon contamination in marine sediments. Marine Chemistry 102, 242-251.

Johnson, S.Y., Alam, A.M.N., 1991. Sedimentation and tectonics of the Sylhet Trough, Bangladesh. Geological Society of America Bulletin 103, 1513-1527.

Kellerman, A.M., Guillemette, F., Podgorski, D.C., Aiken, G.R., Butler, K.D., Spencer, R. G., 2018. Unifying concepts linking dissolved organic matter composition to persistence in aquatic ecosystems. Environmental Science & Technology 52, 2538-2548.

Kemp, A.C., Vane, C.H., Horton, B.P., Engelhart, S.E., Nikitina, D., 2012. Application of stable carbon isotopes for reconstructing salt-marsh floral zones and relative sea level, New Jersey, USA. Journal of Quaternary Science 27, 404-414.

Khan, N.S., Vane, C.H., Horton, B.P., 2015. Stable carbon isotope and C/N geochemistry of coastal wetland sediments as a sea-level indicator. In: Handbook of Sea-Level Research. John Wiley & Sons Ltd, pp. 295-311.

Kister, J., Guiliano, M., Largeau, C., Derenne, S. and Casadevall, E., 1990. Characterisation of chemical structure, degree of maturation and oil potential of Torbanites (type I kerogens) by quantitative FT-ir spectroscopy. Fuel, 69(11), pp.1356-1361.

Kohn, M.J., 2010. Carbon isotope compositions of terrestrial C_3 plants as indicators of (paleo)ecology and (paleo)climate. Proceedings of the National Academy of Sciences of the United States of America 107, 19691-19695.

Kumar, S., Dutta, S. and Bhui, U.K., 2021. Provenance of organic matter in an intracratonic rift basin: Insights from biomarker distribution in Palaeogene crude oils of Cambay Basin, western India. Organic Geochemistry, 162, p.104329.

Kuramoto, T., Minagawa, M., 2001. Stable carbon and nitrogen isotopic characterisation of organic matter in a mangrove ecosystem on the southwestern coast of Thailand. Journal of Oceanography 57, 421-431.

Lafargue, E., Marquis, F., Pillot, D., 1998. Rock-Eval 6 applications in hydrocarbon exploration, production, and soil contamination studies. Revue de l'institut français du p´etrole 53, 421-437.

Laier, T., Jorgensen, N.O., Buchardt, B., Cederberg, T., Kuijpers, A., 1992. Accumulation and seepages of biogenic gas in Northern Denmark. Continental Shelf Research 12, 1173-1186.

Lehmann, M.F., Bernasconi, S.M., Barbieri, A., McKenzie, J.A., 2002. Preservation of organic matter and alteration of its carbon and nitrogen isotope composition during simulated and in situ early sedimentary diagenesis. Geochimica et Cosmochimica Acta 66, 3573-3584.

Li, M.W., Larter, S.R., Taylor, P., Jones, D.M., Bowler, B., Bjorøy, M., 1995. Biomarkers or not biomarkers? A new hypothesis for the origin of pristine involving derivation from methyltrimethyltridecylchromans (MTTCs) formed during diagenesis from chlorophyll and alkylphenols. Organic Geochemistry 23, 159–167.

Lijmbach, W., 1975. On the origin of petroleum. 9th World Petroleum Congress.

Liles, M.R., Williamson, L.L., Rodbumrer, J., Torsvik, V., Parsley, L.C., Goodman, R.M., Handelsman, J., 2009. Isolation and cloning of high molecular weight metagenomic DNA from soil microorganisms. Cold Spring Harbor Protocols 4, 1024-1032.

Littke, R., Leythaeuser, D., 1993. Migration of oil and gas in coals. American Association of Petroleum Geologists Bulletin 38, 219-236.

Luton, P.E., Wayne, J.M., Sharp, R.J., Riley, P.W., 2002. The *mcrA* gene as an alternative to 16S rRNA in the phylogenetic analysis of methanogen populations in landfill. Microbiology 148, 3521-3530.

Madeira, F., Park, Y.M., Lee, J., Buso, N., Gur, T., Madhusoodanan, N., Basutkar, P., Tivey, A.R.N., Potter, S.C., Finn, R.D., Lopez, R., 2019. The EMBL-EBI search and sequence analysis tools APIs in 2019. Nucleic Acids Research 47, W636-W641.

Mauerhofer, L.M., Zwirtmayr, S., Pappenreiter, P., Bernacchi, S., Seifert, A.H., Reischl, B., Schmider, T., Taubner, R.S., Paulik, C., Rittmann, S.K.M., 2021. Hyperthermophilic methanogenic archaea act as high-pressure CH4 cell factories. Communications Biology 4, 1-12.

Meyer, B., Kuever, J., 2007. Molecular analysis of the diversity of sulfate-reducing and sulphur-oxidising prokaryotes in the environment, using aprA as functional marker gene. Applied and Environmental Microbiology 73, 7664-7679.

Meyers, P.A., 1994. Preservation of elemental and isotopic source identification of sedimentary organic matter. Chemical Geology 114, 289-302.

Meyers, P.A., 1997. Organic geochemical proxies of paleoceanographic, paleolimnologic and paleoclimatic processes. Organic Geochemistry 27, 213-250.

Meyers, P.A., Ishiwatari, R., 1993. Lacustrine organic geochemistry-an overview of indicators of organic matter sources and diagenesis in lake sediments. Organic Geochemistry 20, 867-900.

Meyers, P.A., Teranes, J.L., 2001. Sediment organic matter. In: Last, W.M., Smol, J.P. (Eds.), Tracking Environmental Change using Lake Sediments, Physical and Geochemical Methods, vol. 2. Kluwer Academic Publishers, Dordrecht, pp. 239-269.

Middelburg, J.J., Herman, P.M.J., 2007. Organic matter processing in tidal estuaries. Marine Chemistry 106, 127-147.

M¨obius, J., Lahajnar, N., Emeis, K.C., 2010. Diagenetic control of nitrogen isotope ratios in Holocene sapropels and recent sediments from the Eastern Mediterranean Sea. Biogeosciences 7, 3901-3914.

Morgan, J.P., McIntire, W.G., 1959. Quaternary geology of the Bengal Basin (East Pakistan and India). Geological Society of America Bulletin 70, 319-342.

Mukherjee, A., Fryar, A.E., Thomas, W.A., 2009. Geologic, geomorphic and hydrologic framework and evolution of the Bengal basin, India and Bangladesh. Journal of Asian Earth Sciences 34, 227-244.

Najman, Y., Bickle, M., BouDagher-Fadel, M., Carter, A., Garzanti, E., Paul, M., Wijbrans, J., Willett, E., Oliver, G., Parrish, R., Akhter, S.H., Allen, R., Ando, S., Chisty, E., Reisberg, L., Vezzoli, G., 2008. The Paleogene record of Himalayan erosion: Bengal Basin, Bangladesh. Earth and Planetary Science Letters 273, 1-14.

Nguyen, R.T., Harvey, H.R., 1997. Protein and amino acid cycling during phytoplankton decomposition in oxic and anoxic waters. Organic Geochemistry 27, 115–128.

Natelhoffer, K.J., Fry, B., 1988. Controls on natural nitrogen-15 and carbon-13 abundances in forest soil organic matter. Soil Science Society of America 52, 1633-1640.

Ogbesejana, A.B., Liu, B., Ostadhassan, M., 2021. Stable Isotope Geochemistry of the Organic Elements within Shales and Crude Oils: A Comprehensive Review. Molecules, 27, p.34.

Ortiz, J.E., Moreno, L., Torres, T., Vegas, J., Ruiz-Zapata, B., Garcia-Cortes, A., Galan, L., Perez-Gonzalez, A., 2013. A 220 ka paleoenvironmental reconstruction of the Fuentillejo maar lake record (central Spain) using biomarker analysis. Organic Geochemistry 55, 85-97.

Peters, K.E., 1986. Guidelines for evaluating petroleum source rock using programmed pyrolysis. American Association of Petroleum Geologists Bulletin 70, 318-386.

Peters, K.E., Clark, M.E., Das Gupta, U., McCaffrey, M.A., Lee, C.Y., 1995. Recognition of an infraCambrian source rock based on biomarkers in the Bagehwala-1 oil, India. American Association of Petroleum Geologists Bulletin 79, 1481-1494.

Peters, K.E., Fraser, T.H., Amris, W., Rustanto, B., Hermanto, E., 1999. Geochemistry of crude oils from eastern Indonesia. American Association of Petroleum Geologists Bulletin 83, 1927-1942.

Peters, K.E., Walters, C.C., Moldowan, J.M., 2005. The Biomarker Guide. Biomarkers and Isotopes in the Environment and Human History. Cambridge University Press, New York. Chapter 4.

Ramaswamy, G., 1962. Aeromagnetic and gravity surveys of West Bengal. In: Proceedings of the Seminar on oil prospects in the Ganga Valley. Oil and Natural Gas Corporation, Dehradun, pp. 28-29.

Ramaswamy, V., Gaye, B., Shirodkar, P.V., Rao, P.S., Chivas, A.R., Wheeler, D., Thwin, S., 2008. Distribution and sources of organic carbon, nitrogen and their isotopic signatures in sediments from the Ayeyarwady (Irrawaddy) continental shelf, northern Andaman Sea. Marine Chemistry 111, 137-150.

Rea, D.K., 1992. Delivery of the Himalayan sediments to the Northern Indian Ocean and its relation to global climate, sea-level, uplift and seawater strontium. In: Duncan, R.

Rice, P., Longden, I., Bleasby, A., 2000. EMBOSS: the European molecular biology open software suite. Trends in Genetics 16, 276-277.

Rieley, G., Collier, R.J., Jones, D.M., Eglinton, G., Eakin, P.A., Fallick, A.E., 1991. Sources of sedimentary lipids deduced from stable carbon-isotope analyses of individual compounds. Nature 352, 425-427.

Rontani, J.F., Bonin, P., 2011. Production of pristane and phytane in the marine environment: role of prokaryotes. Research in Microbiology 162, 923-933.

Roybarman, A., 1984. Geology and hydrocarbon prospects of West Bengal. Petroleum Asia Journal 6, 51-56.

Sakata, S., Hayes, J.M., McTaggart, A.R., Evans, R.A., Leckrone, K.J., Togasaki, R.K., 1997. Carbon isotopic fractionation associated with lipid biosynthesis by a cyanobacterium: relevance for interpretation of biomarker records. Geochimica et Cosmochimica Acta 61, 5379-5389.

Schelske, C.L., Hodell, D.A., 1995. Using carbon isotopes of bulk sedimentary organic matter to reconstruct the history of nutrient loading and eutrophication in Lake Erie. Limnology and Oceanography 409, 918-929.

Sengupta, S., 1966. Geological and geophysical studies in the western part of Bengal Basin, India. American Association of Petroleum Geologists Bulletin 50, 1001-1017.

Shamsuddin, A.H.M., Khan, S.I., 1991. Geochemical criteria of migration of natural gases in the Miocene sediments of the Bengal Foredeep, Bangladesh. Journal of Southeast Asian Earth Sciences l5, 89-100.

Silliman, J.E., Meyers, P.A., Bourbonniere, R.A., 1996. Record of postglacial organic matter delivery and burial in sediments of Lake Ontario. Organic Geochemistry 24, 463-472.

Silverman, S.R., 1965. Migration and segregation of oil and gas fluids in subsurface environments. American Association of Petroleum Geologists Memoir 4, 54-65.

Sivan, P., Datta, G.C., Singh, R.R., 2008. Aromatic biomarkers as indicators of source, depositional environment, maturity and secondary migration in the oils of Cambay Basin, India. Organic Geochemistry, 39(11), pp.1620-1630.

Tareq, S.M., Tanoue, E., Tsuji, H., Tanaka, N., Ohta, K., 2005. Hydrocarbon and elemental carbon signatures in a tropical wetland: biogeochemical evidence of forest fire and vegetation changes. Chemosphere 59, 1655-1665.

ten Haven, H.L., de Leeuw, J.W., Rullk¨otter, J., Sinninghe Damst´e, J.S., 1987. Restricted utility of the pristane/phytane ratio as a palaeoenvironmental indicator. Nature 330, 641-643.

Teranes, J.L., Bernasconi, S.M., 2000. The record of nitrate utilisation and productivity limitation provided by $\delta^{15}N$ values in lake organic matter—A study of sediment trap and core sediments from Baldeggersee, Switzerland. Limnology and Oceanography 45, 801-813.

Thode, H.G., 1981. Sulfur isotope ratios in petroleum research and exploration: Williston Basin. American Association of Petroleum Geologists Bulletin 65, 1527-1535.

Tissot, B.P., Welte, D.H., 1984. Petroleum Formation and Occurrence, second ed. Springer-Verlag, Berlin.

Tringe, G.S., Rubin, E.M., 2005. Metagenomics: DNA sequencing of environmental samples. Nature Reviews Genetics 6, 805-814.

Uddin, A., 1990. Shift in depositional patterns during Miocene time in the Bengal Basin, Bangladesh. Geological Society of America Program with Abstracts 22, A366.

Uddin, A., Lundberg, N., 1998. Cenozoic history of the Himalayan-Bengal system: sand composition in the Bengal basin, Bangladesh. Geological Society of America Bulletin 110, 497-511.

Volkman, J.K., Barrett, S.M., Blackburn, S.I., Mansour, M.P., Sikes, E.L., Gelin, F., 1998. Microalgal biomarkers: a review of recent research developments. Organic Geochemistry 29, 1163-1179.

Walker, D.I., McComb, A.J., 1985. Decomposition of leaves from *Amphibolis Antarctica* (Labill.) Sonder ex Aschers. and *Posidonia australis* Hook. f. the major seagrasses of Shark Bay. Western Australia. Botanica Marina 28, 407-413.

Weber, ME., Lantzsch, H., Dekens, P., Das, SK., Reilly, B., Martoc, YM., Meyer-Jacob, C., Agrahari, S., Ekblad, A., Titschack, J., Holmes, B., Wolfgramm, P., 2018. 200,000 years of monsoonal history recorded on the lower Bengal Fan—strong response to insolation forcing. Global Planet Change 166, 107–119

Wei, Z., Walters, C.C., Moldowan, J.M., Mankiewicz, P.J., Pottorf, R.J., Xiao, Y., Maze, W., Nguyen, P.T., Madincea, M.E., Phan, N.T., Peters, K.E., 2012. Thiadiamondoids as proxies for the extent of thermochemical sulfate reduction. Organic Geochemistry 44, 53-70.

Wu, W., Ruan, J., Ding, S., Zhao, L., Xu, Y., Yang, H., Ding, W., Pei, Y., 2014. Source and distribution of glycerol dialkyl glycerol tetraethers along lower Yellow Riverestuary–coast transect. Marine Chemistry 158, 17–26.

Wynn, J.G., Bird, MI, 2007. C_4-derived soil organic carbon decomposes faster than its C_3 counterpart in mixed C_3/C_4 soils. Global Change Biology 13, 2206-2217.

Xing, L., Zhang, H., Yuan, Z., Sun, Y., Zhao, M., 2011. Terrestrial and marine biomarker estimates of organic matter sources and distributions in surface sediments from the East China Sea shelf. Continental Shelf Research 31, 1106-1115.

Yakimovich, K.M., Emilson, E.J., Carson, M.A., Tanentzap, A.J., Basiliko, N., Mykytczuk, N., 2018. Plant litter type dictates microbial communities responsible for greenhouse gas production in amended lake sediments. Frontiers in Microbiology 2662.

Yakimovich, K.M., Orland, C., Emilson, E.J., Tanentzap, A.J., Basiliko, N., Mykytczuk, N., 2020. Lake characteristics influence how methanogens in littoral sediments respond to terrestrial litter inputs. The ISME Journal 14, 2153-2163.

Yeh, H.W., Epstein, S., 1981. Hydrogen and carbon isotopes of petroleum and related organic matter. Geochimica et Cosmochimica Acta 45, 753-762.

Zhang, Z., Zhao, M., Yang, X., Wang, S., Jiang, X., Oldfield, F., Eglinton, G., 2004. A hydrocarbon biomarker record for the last 40 kyr of plant input to Lake Heqing, southwestern China. Organic Geochemistry 35, 595-613.